

Combo: Co-speech holistic 3D human motion generation and efficient customizable adaptation in harmony

Chao Xu, Mingze Sun, Zhi-Qi Cheng, Fei Wang, Yang Liu, Baigui Sun, Ruqi Huang, Alexander Hauptmann

Abstract—In this paper, we propose a novel framework, `Combo`, for harmonious co-speech holistic 3D human motion generation and efficient customizable adaption. In particular, we identify that one fundamental challenge as the multiple-input-multiple-output (MIMO) nature of the generative model of interest. More concretely, on the input end, the model typically consumes both speech signals and character guidance (*e.g.*, identity and emotion), which hinders further adaptation to varying guidance; on the output end, holistic human motions mainly consist of facial expressions and body movements, which are inherently correlated but non-trivial to coordinate in current data-driven generation process. In response to the above challenge, we propose tailored designs to both ends. For the former, we propose to pre-train on data regarding a fixed identity with neutral emotion, and defer the incorporation of customizable conditions (identity and emotion) to fine-tuning stage, which is boosted by our novel x -Adapter for parameter-efficient fine-tuning. For the latter, we propose a simple yet effective transformer design, DU-Trans, which first divides into two branches to learn individual features of face expression and body movements, and then unites those to learn a joint bi-directional distribution and directly predicts combined coefficients. Evaluated on BEAT2 and SHOW datasets, `Combo` is highly effective in generating high-quality motions but also efficient in transferring identity and emotion. Project website: [Combo](#).

Index Terms—Co-speech Holistic 3D Human Motion Generation, Parameter-Efficient Fine-Tuning, Diffusion Models



1 INTRODUCTION

In this paper, we study the problem of co-speech holistic 3D human motions generation [1], namely, given speech signal and character conditions (*e.g.*, identity, emotion), generating facial expressions and body movements including hand gestures and body motions. This generation task is crucial in crafting digital avatars as it significantly enhances the interaction informativeness and vividness of the latter [2], [3], therefore attracting increasing interest from generative AI research.

One fundamental challenge of this task stems from its multi-input-multi-output (MIMO) nature: 1) the input end gathers not only various factors including speech contents, rhythms, and semantics, but also character conditions like identities and emotions; 2) the output end delivers both facial and body motions, which are inherently related but non-trivial to align. For humans, such a perplexing system is well governed by a nervous system, yielding harmonious, adaptive (*e.g.*, regarding emotion changes) holistic motions in real life. On the other hand, generative models typically take a data-driven approach to learning from human videos. While

being straightforward, it is highly non-trivial to learn the inherent relationships within the MIMO system purely from data.

In light of the above, we examine the holistic human motion generation task from a principled perspective and advocate two novel designs tailored for improving data-driven generative model. Our key insight is to alleviate modeling complexity in both input and output end, leading to a *harmonious but also adaptive* generative network. For the input end, instead of training an encoder that consumes all at once, we pre-train a model in a relatively clear setting, and defer the injection of important conditions to the fine-tuning stage; For the output end, we propose a divide-and-unite strategy to address the trade-off between learning accurate facial and body movements and guaranteeing coherence. In the following, we motivate and explain the above designs in more detail.

Regarding the **multiple input end**, our generative model is expected to take speeches as generation guidance, which contain factors such as contents, rhythms, semantics, and so on. It is worth noting that the same speech guidance can lead to different motion sequences with respect to varying conditions (*e.g.*, identity and emotion), complicating the learning process. The significant contributions to high-quality dataset construction [3], [5], containing rich annotations as well as great variability in identity and emotions, offer good opportunities for learning a comprehensive model. However, we argue that learning a comprehensive model lacks flexibility in further adaptation. In fact, generative models have been widely desired to be controllable and customizable [6], [7], [8], [9]. Regarding holistic human motion generation, one would naturally expect a flexible, adaptive digital avatar with respect to changes in both short-term emotional states (emotion) and long-term personality (identity). Unfortunately, recent efforts [1], [2], [3], [10], [11] require an extensive training or full-

- C. Xu, F. Wang, Y. Liu and B. Sun are with Alibaba Group (e-mail: {xc264362, steven.wf, ly261666}@alibaba-inc.com, sun-baigui85@gmail.com).
- C. Xu is with Zhejiang Univeristy (e-mail: 21832066@zju.edu.cn).
- M. Sun, and R. Huang are with Tsinghua Shenzhen International Graduate School, Tsinghua University (e-mail: smz22@tsinghua.edu.cn, ruqi-huang@sz.tsinghua.edu.cn).
- Z. Cheng, and H. Alexander are with Carnegie Mellon University (e-mail: {zhiqic, alex@cs.cmu.edu}).
- C. Xu, M. Sun, Z. Cheng are equal technical contribution. This work was completed in collaboration with Carnegie Mellon University.

Manuscript received April 19, 2005; revised August 26, 2015.

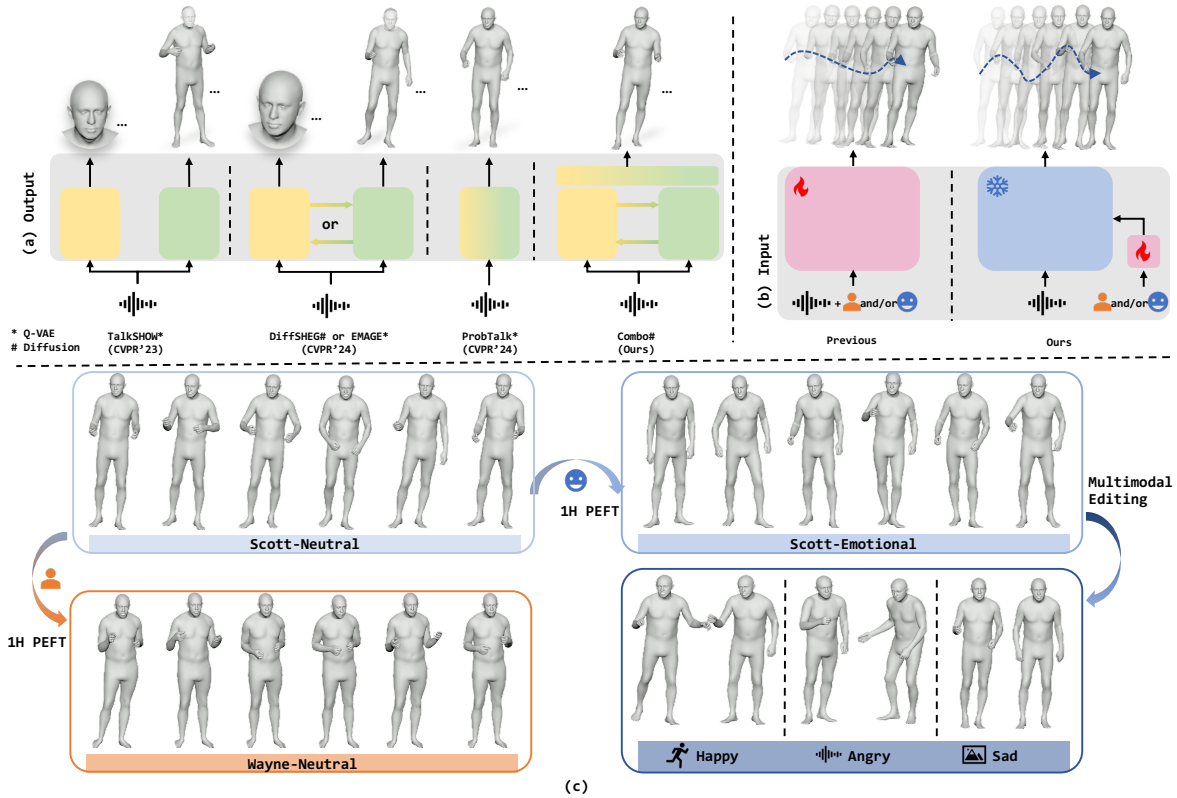


Fig. 1. An illustrative comparison of SOTA methods and our approach. (a) On output end, TalkSHOW [1] adopts two separate networks to predict audio-synchronized expressions and gestures, thus leading to a disjointed issue. Subsequent work [2], [3] only account for bidirectional interaction and use two heads predict independently, still leading to a risk of disharmony. ProbTalk [4] directly learns holistic motion for harmony but the specificity of each component is lost. Conversely, our method not only achieves *holistic harmony* but also maintains *individual uniqueness*. (b) On input end, previous works typically learn a comprehensive model to fit the multiple inputs, including audio signals and other conditions. Thus they require training or finetuning the entire network for different conditions. In contrast, we pre-train a model in a relatively clear setting, and adapt various conditions in the fine-tuning stage. Our design allows flexible and efficient adaptation (*1 Hour PEFT*) for identity customization and emotion transfer, as depicted in part (c). Notably, we only utilize the embeddings from emotional text prompts encoded by CLIP as guidance during training. At inference, other modalities such as motion clips, audios, and images can all serve as emotional conditions, thereby supporting flexible multi-modal editing, as depicted in part (c).

parameter fine-tuning process to accommodate to the emotional data or newly introduced identities, a limitation that is particularly exacerbated in VQ-VAE-based methods [1], [3], as shown in Fig. 1(b).

Motivated by the above observations, we take a pre-train-and-fine-tune approach. During pre-training, we train a model with data from a fixed identity in neutral emotion. The injection of specific conditions, such as alternative identities and/or emotions, is deferred to the fine-tuning stage. Our key design in this part is a novel plug-and-play adapter for Parameter-Efficient Fine-Tuning (PEFT) [12], X-Adapter, which is tailored to our pipeline and allows for effective and efficient fine-tuning on emotion transfer and personalized generation. Our treatment on input end admits several advantages: 1) It alleviates the learning burden during pre-train stage, therefore improving the performance; 2) Built upon the advanced pre-training, the fine-tuning phase can achieve superior performance with minimal computational cost; 3) As a by-product, it further enables versatile editing during inference benefiting from flexible X cues, which is a capability that previous approaches [1], [2], [3] could not attain. For instance, we can employ multi-modal conditions within the CLIP domain [13] to indicate the short-term emotion, which supports flexible and generalizable zero-shot editing. We can also define identity codes as several interpretable statistics of SMPLX [14] to depict long-term personality.

Regarding the **multiple output end**, holistic human motion involves both facial expressions and body movements with different patterns [2], [3], [15], presents a dual challenge: direct holistic modeling [4] is difficult to maintain uniqueness, while separate modeling struggles to generate harmonious full-body natural movements. For the former, ProbTalk [4] directly models the holistic motions for coordination but fails to learn accurate individual distribution. For the latter, TalkSHOW [1] completely ignores the interconnection and results in disjointed coordination among different motion components. Subsequent works [2], [3] identify this discrepancy and explicitly utilize a unidirectional flow between face and body to enhance the correlation. However, the current arts are inadequate to achieve holistic harmony yet individual distinctive, leaving sufficient room for improvement, as shown in Fig. 1(a).

To this end, we propose a simple yet effective transformer design, **DU-Trans**, which first **D**ivides into two branches to learn individual features of face expression and body movements, and then **U**nites those to learn a joint bi-directional distribution and directly predicts combined coefficients by a single output head. Our treatment on the output end enjoys three-fold benefits: 1) By imposing supervision on the individual branches, it respects the distinctiveness between the two and ensures high-quality feature learning; 2) The learned features enable bi-directional communi-

cation between branches in the latent space, fully exploiting the modeling capacity and facilitating the cost of association in the explicit space [2]; 3) The final unification allows for a single-head generation, further enhancing the overall harmony on top of jointly learned features from each branch. Last but not least, combined with our design on the input end, DU-Trans also enables more harmonious customizable adaption.

To conclude, we have established `Combo`, a novel framework for co-speech holistic 3D human motion generation and efficient customizable adaption, both in harmony. Interestingly, our framework echoes its aberration – like a jazz band, it emphasizes harmony during training and inference (practice and play). Moreover, a well-trained jazz band can promptly incorporate with a new leader and/or play a new song with proper rehearsal. Similarly, `Combo` can be adapted to new identities (leader) and/or emotions (a genre of songs) with efficient fine-tuning (rehearsing) as well. To validate the above, we comprehensively perform both quantitative and qualitative evaluations in BEAT2 [3] and SHOW [1] datasets. Our proposed `Combo` is highly effective in generating harmonious motions but also efficient in identity and emotion adaptation, *i.e.*, our results significantly outperform others on the holistic metric FMD and also attain state-of-the-art performance in one-hour fine-tuning (about 5% of the time required for training from scratch) with only updates about 10% parameters.

In summary, our technical contributions are as follows:

- We reexamine the MIMO nature of co-speech holistic 3D human motion generation and focus on reducing its complexity for a harmonious and adaptive framework.
- We propose DU-trans, which first captures the unique characteristics of the face and gesture for synchronization, then learns the joint distribution of them and directly predicts the combined coefficients for harmony.
- We propose X-Adapter, which facilitates the fast and seamless adaptation of a pretrained neutral talking body to stylized versions or other different identities.
- Extensive experiments on SHOW [1] and BEAT2 [5] datasets confirm that our approach can realize the SOTA performance. Detailed analysis validates the superiority of our method in motion quality and transfer efficiency.

2 RELATED WORK

2.1 Speech-Driven Body Motion Generation

Holistic body motion generation from speech [1], [2], [3], [4], [15], [16] encompasses the coordinated creation of movements for three key body parts: the face, hands, and body. However, most efforts only consider parts of the human body rather than the holistic body. For speech-driven facial movement generation, it is often referred to as talking face generation [17], [18], [19], [20], [21], whether in 2D or 3D, is a vibrant field that involves creating animated faces that can mimic human speech and expressions. Recent 3D facial animation leverage blendshapes [20], [22], [23] or 3D meshes [21], [24], [25] as the structure representation to control the lip shapes and capture speech nuances. Considering the complexity of mapping speech to facial expressions, probabilistic models such as VQ-VAE [1], [26], [27], [28] and diffusion models [29], [30], [31], [32], [33], [34] have been employed to predict the distribution of facial expressions derived from speech signals. Similarly, methods for speech-driven gesture generation [5], [11], [35], [36], [37], [38], [39], [40] are also designed to estimate the

mapping or probability distribution of body and hand motion with the help of various condition modalities, including acoustic features, linguistic characteristics, speaker identities, and emotions.

Recently, Habibie *et al.* [41] first utilized a CNN-based framework to generate 3D facial meshes and 3D key points of the body and hands simultaneously. However, they overlook the coordination between body parts, and at the same time, deterministic models also lead to a lack of diversity. Thus, subsequent works all resort to a generative model to incorporate diversity into motion generation. TalkSHOW [1] is built upon the VQ-VAE and designs a cross-conditioned mechanism between the body and hand motions to keep the synchronization of the gesture, but they treat facial expression estimation as an independent task. To address the coordination issue between expression and gestures, DiffSHEG [2] and EMAGE [3] divide two encoders, one for expression and one for gesture, and establish a path for unidirectional information flow between each. ProbTalk [4] jointly models the holistic motion with the help of PQ-VAE [42] in a unified manner. Nevertheless, current methods fail to learn harmonious relationships between various body parts while maintaining the unique distribution of each. In our work, we explore the feasibility of this by a divide and unite mechanism for highly synchronized and coordinated full-body motions. Moreover, existing approaches [1], [2], [3] typically require the definition of identities and emotions during training to guide the learning of specific characteristics. When the network encounters unseen identities and emotional styles, it may fail to generalize effectively, necessitating complete retraining or fine-tuning of the network with additional data to accommodate new conditions. In contrast, we introduce an efficient adaptation strategy that converts a pretrained model into various customized ones, enhancing the flexibility and applicability of our approach.

2.2 Parameter-Efficient Fine-Tuning

Unlike conventional fine-tuning, which updates all parameters, Parameter-Efficient Fine-Tuning (PEFT) has shown impressive results across various tasks by updating only a subset of parameters. The three primary methods of PEFT are Adapter [43], [44], prefix-tuning [45], [46], and LoRA [47], [48]. In the realm of NLP, the concept of adapters was first introduced by the Serial Adapter [49] model. This model enhances each Transformer block by incorporating two additional adapter modules, one after the self-attention layer and the other after the feed-forward neural network (FFN) layer. Parallel Adapter [50], on the other hand, restructures these sequential layers into a parallel side network that operates in tandem with each Transformer sublayer. Our X-Adapter is largely based on this concept. With the growing interest in diffusion models [29], [51], recent studies have applied PEFT to refine pre-trained diffusion models for specialized tasks. We introduce two key applications, including integrating additional input modalities and customizing content generation. Specifically, GLIGEN [52] integrates new trainable gated Transformer layers without altering the original model’s weights, while ControlNet [53] fine-tunes a separate encoding layer copy from Stable Diffusion [51] while locks its pre-trained parameter weights. T2I-Adapter [54] adds a lightweight model to synchronize external controls with the model’s internal processes. For customization, Textual Inversion [55] identifies pseudo-words for concept representation, and IP-Adapter [56] inserts an image-focused attention layer for feature enhancement. Notably, EAT [57] employs a pre-train-and-fine-tune approach similar to ours, but they extend a

trainable encoder branch for fine-tuning directly, which is neither as efficient nor as effective as PEFT. In this work, we integrate PEFT into the domain of holistic 3D human motion generation for flexible adaptation, which is the first attempt in this field.

3 METHOD

Our proposed `Combo` framework aims to deliver harmonious holistic motion generation as well as efficient customizable adaptation with respect to new identity and/or emotion. Before diving into technical details, we first give a preliminary overview on holistic human motion generation in Section 3.1. Then we introduce DU-Trans in Section 3.2, which is key to creating synchronized and coordinated full-body talking motions. After that, we introduce X-Adapter for efficient emotion style transfer and rapid personalization in Section 3.3. Finally, we describe how X-Adapter can be used for conditional editing in Section 3.4

3.1 Preliminary

Holistic Human Shape Model. Following [1], [2], [3], we use SMPLX [14] as generation representation, which is a well-known parametric model for characterizing holistic expressive human shapes, including detailed facial expression, hand gesture and body pose. This model is widely utilized in computer graphics and virtual reality, providing a high degree of realism and flexibility for character creation and motion animation. Starting with a template mesh consisting of n vertices and a fixed triangulation, SMPLX associates parameters and human shapes via function $M(\rho, \omega, \psi) : \mathbb{R}^{|\rho|+|\omega|+|\psi|} \rightarrow \mathbb{R}^{3n}$. Namely, given a set of parameters (ρ, ω, ψ) , the function returns coordinates of a human shape in a fixed order, which, together with the pre-fixed triangulation, forms a plausible human mesh. The parameters carry different semantics: identity $\rho \in \mathbb{R}^{300}$ captures the specific shape characteristics of the body; pose $\omega \in \mathbb{R}^{J \times 3}$ encodes rotations around a defined set of joints ($J = 55$), which allows details as intricate as finger articulation; facial expression $\psi \in \mathbb{R}^{100}$ represents a wide array of facial movements for expressive animations. Thanks to SMPLX, we can cast holistic human motion generation as the respective parameter generation.

Diffusion Models. Our approach employs diffusion models, encompassing diffusion and denoising stages. With a given distribution of motion clips, our objective is to train a model with parameters θ to approximate the initial state $\mathbf{x}_0^{1:N}$ (noise-free sequence of $\mathbf{x}^{1:N}$, N is the sequence length). During the diffusion phase, the model incrementally degrades the input data $\mathbf{x}_0^{1:N} \sim p(\mathbf{x}_0^{1:N})$ following a set schedule $\beta_t \in (0, 1)$, culminating in an isotropic Gaussian distribution across T steps. Each step of the forward transition can be represented as:

$$q(\mathbf{x}_t^{1:N} | \mathbf{x}_{t-1}^{1:N}) = \mathcal{N}(\mathbf{x}_t^{1:N}; \sqrt{1 - \beta_t} \mathbf{x}_{t-1}^{1:N}, \beta_t \mathbf{I}). \quad (1)$$

Conversely, in the denoising phase, the model is trained to reverse the noising process, thereby converting noise back into the actual data distribution during inference. The backward transition is:

$$p_\theta(\mathbf{x}_{t-1}^{1:N} | \mathbf{x}_t^{1:N}) = \mathcal{N}(\mathbf{x}_{t-1}^{1:N}; \mu_\theta(\mathbf{x}_t^{1:N}, t), \Sigma_\theta(\mathbf{x}_t^{1:N}, t)). \quad (2)$$

We follow Ho *et al.* [29] to model the mean $\mu_\theta(\mathbf{x}_t^{1:N}, t)$ of the reverse distribution while keeping the variance $\Sigma_\theta(\mathbf{x}_t^{1:N}, t)$ fixed. Instead of predicting the noise ϵ_t , we follow Ramesh *et al.* [58] and predict the signal $\hat{\mathbf{x}}_0^{1:N}$ itself with the simple objective [29]:

$$\mathcal{L}_{\text{simple}} = \mathbb{E}_{t, \mathbf{x}_0} [\mathbf{x}_0^{1:N} - \hat{\mathbf{x}}_0^{1:N}]. \quad (3)$$

Adapters [49] are one of the state-of-the-art techniques in Parameter-Efficient Fine-Tuning (PEFT), implemented by embedding compact, auxiliary layers into the Transformers. The adapter layer typically compresses the input \mathbf{h} into a lower-dimensional space via a down-projection with matrix $\mathbf{W}_{\text{down}} \in \mathbb{R}^{d \times r}$, constrained by the bottleneck dimension r to minimize parameter count. It then applies a non-linear activation function $\delta(\cdot)$, before expanding the features back with an up-projection using $\mathbf{W}_{\text{up}} \in \mathbb{R}^{r \times d}$. This bottleneck module is connected to the original pre-trained models through the residual connection.

3.2 DU-Trans

Fig. 2(a) shows an illustration of DU-Trans. In the following, we begin by describing the extraction of comprehensive audio features. Then we present details of the network architecture. Finally, we introduce the training loss terms.

Audio Feature Extraction. In this part, we follow the common practice [59], [60] to decompose input speech signal into content, rhythm, and semantics. As suggested by recent progress [15], the local lip motion is strongly correlated with the input audio content, and the global facial expression is related to the audio rhythm. While the body has a weaker correlation with the content, yet is intricately connected to audio semantics and rhythm [61]. Early approach [1] leverages MFCC [62] to encode speech, which falls short of capturing rich speech information and struggles with disentangling each component. Therefore, we resort to recent advances in audio pre-trained models. Specifically, we use wav2vec 2.0 [63] trained on Automatic Speech Recognition (ASR) task as our audio content extractor, obtaining $\mathbf{A}_c^{1:N} \in \mathbb{R}^{1024 \times N}$, which primarily retains the phonemes and filters out irrelevant information. Regarding rhythm, we choose the JDC network [64] trained on LibriSpeech [65] to predict acoustic rhythm $\mathbf{A}_r^{1:N} \in \mathbb{R}^{1 \times N}$. For semantics, we first follow [61] to align words with the corresponding speech and convert the text into frame-level features (SHOW [1] dataset requires this processing while BEAT2 [5] does not). Then we take the aligned text as input and use the pretrained model of BERT [66] to encode $\mathbf{A}_s^{1:N} \in \mathbb{R}^{1536 \times N}$.

Architecture. Given the markedly different audio-related dynamics of facial expressions and gestures, it is essential to independently model these components for enhanced synchronization. However, this approach alone risks neglecting the intrinsic connections between them and could cause disjointed coordination. Previous works [2], [3] have recognized this issue, but they only introduce uni-flow and use multiple heads to predict individual coefficients still hindering overall coordination. In contrast, we propose a divide-and-unite strategy that respects the distinct modeling needs of each component while implicitly accounting for their interrelationships and directly predicting a unified set of coefficients, thus possessing synchronization and coordination in a unified framework. Specifically, we combine this strategy with a diffusion model. As shown in Fig. 2(a), we first implement four key designs to learn the distinct dynamic characteristics of the face and body:

- 1) Two separate Transformer encoders Ψ^F, Ψ^B are employed to respectively model the features of face and body, allowing for specialized feature modeling for face and body movements;
- 2) Each branch is designed to receive features with which it has a strong correlation. The face branch takes as input audio content $\mathbf{A}_c^{1:N}$, rhythm $\mathbf{A}_r^{1:N}$, and noise face sequences $\mathbf{F}_t^{1:N}$, with

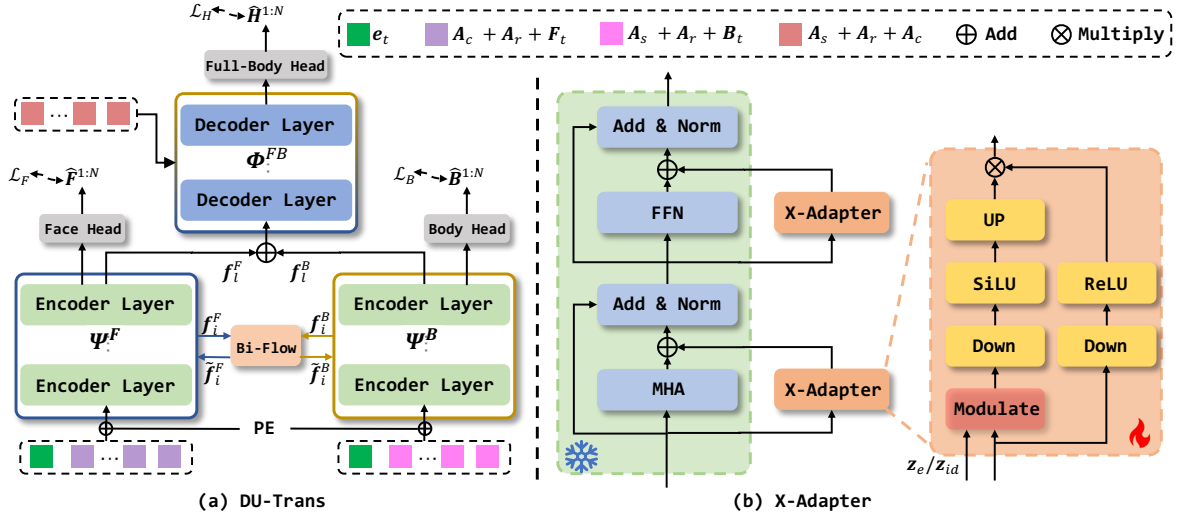


Fig. 2. **Architecture overview of Combo.** The basic architecture named DU-Trans (a) first introduces two transformer encoders Ψ^F , Ψ^B incorporated with auxiliary losses \mathcal{L}_F , \mathcal{L}_B and Bi-Flow to help model their respective distributions, obtaining two sets of discriminative features f_l^F , f_l^B . Subsequently, it merges these two features and inputs them into the decoder Φ^{FB} to learn the joint distribution, and directly uses a single head to predict synchronized and coordinated face and body coefficients. Then, X-Adapter (b) is the central module for achieving identity customization and emotion transfer, and it is simply inserted in parallel into the MHA and FFN layers of the two encoders. Note that this adapter is a general structure suitable for both identity and emotion, offering better controllable generation through conditions z_e and z_{id} .

time-step information e_t also integrated into the input sequence. Formally:

$$f_l^F = \Psi^F(\text{PE} + [e_t, A_c^{1:N} + A_r^{1:N} + F_t^{1:N}]), \quad (4)$$

where $[\cdot]$ means concatenation, l is the number of encoder layers, and PE is the positional embedding. The body branch, on the other hand, receives semantic information rather than phonetic content:

$$f_l^B = \Psi^B(\text{PE} + [e_t, A_s^{1:N} + A_r^{1:N} + B_t^{1:N}]). \quad (5)$$

3) A Bi-Flow layer built upon the cross-attention mechanism is introduced to preliminarily model the relationship between the two branches, capturing holistic dynamic priors to enhance the performance of each component. We take face to body data-flow for example, the query Q_B is extracted by linear projection from f_i^B (i is the layer index), and the key and value K_F , V_F is extracted from f_i^F in the same way. To obtain the updated body feature \tilde{f}_i^B ,

$$f_i^{F \rightarrow B} = \text{softmax}\left(\frac{Q_B(K_F)^T}{\sqrt{d}}\right)V_F, \quad (6)$$

$$\tilde{f}_i^B = \text{MLP}(\text{LN}(f_i^{F \rightarrow B})) + f_i^B, \quad (7)$$

where MLP and LN is a MLP block and a LayerNorm, \sqrt{d} is a scaling factor.

4) Our architecture consists of three output heads: Two output heads are used to predict independent coefficients for face and body under auxiliary supervisions (*c.f.* Loss Functions paragraph below); One output head is for holistic generation. By summing the face features f_l^F and body features f_l^B output by the two encoders and feeding the sum into the single decoder Φ^{FB} to implicitly model their interrelations, During training, all output heads are optimized with regarding training loss, while during inference only the last head is activated to deliver coordinated holistic human motions. Formally,

$$f^{FB} = \Phi^{FB}(f_l^F + f_l^B, A_s^{1:N} + A_r^{1:N} + A_c^{1:N}). \quad (8)$$

Loss Functions. During the training phase, our model outputs three predicted parameters: facial expression $\hat{F}^{1:N} \in \mathbb{R}^{N \times 100}$ and body gestures $\hat{B}^{1:N} \in \mathbb{R}^{N \times 165}$ output from two encoder, and the combined one $\hat{H}^{1:N} \in \mathbb{R}^{N \times 265}$ output from a single decoder. Each is supervised by two loss functions, simple loss $\mathcal{L}_{\text{simple}}$ following the Eq. 3 and velocity loss \mathcal{L}_{vel} . Formally, we take the holistic body as an example:

$$\mathcal{L}_{\text{vel}} = \frac{1}{N-1} \sum_{i=1}^{N-1} \left\| (H^{i+1} - H^i) - (\hat{H}^{i+1} - \hat{H}^i) \right\|_2^2, \quad (9)$$

$$\mathcal{L}_{\text{simple}} = \mathbb{E}_{t, H} \left[H^{1:N} - \hat{H}^{1:N} \right], \quad (10)$$

$$\mathcal{L}_H = \mathcal{L}_{\text{vel}} + \mathcal{L}_{\text{simple}}. \quad (11)$$

Overall, our training loss is:

$$\mathcal{L} = \mathcal{L}_H + \lambda_F \mathcal{L}_F + \lambda_B \mathcal{L}_B, \quad (12)$$

where λ_F and λ_B are set to 0.5 and 0.5, respectively. \mathcal{L}_F and \mathcal{L}_B serve as two auxiliary losses during training.

3.3 x-Adapter

In this section, we present X-Adapter, as shown in Fig. 2(b) and Alg. 1, for efficient fine-tuning.

Architecture. Based on the vanilla adapter [49] described in Sec. 3.1, we make some modifications and propose the X-Adapter.

1) To balance the task-agnostic features generated by the original frozen branch and the task-specific features generated by the tunable bottleneck branch, we do not rely on a simple scalar hyperparameter as a scale. Instead, we adopt a parallel down-projection layer with matrix $W_s \in \mathbb{R}^{d \times 1}$ to dynamically generate a scale factor, named Dy-Scale $s_d \in \mathbb{R}^N$ based on the input motion sequences. Importantly, we follow this with a ReLU activation to select the positive scale and set the rest to zero. Because only significant local motion tokens require adjustment during fine-tuning, it should depend on the unique characters of each input feature:

$$s_d = \text{ReLU}(W_s h). \quad (13)$$

Algorithm 1 PyTorch-like code of X-Adapter.

```

import torch.nn as nn
class XAdapter(nn.Module):
    def __init__(self, rank, d_model):
        super().__init__()
        self.down_proj = nn.Linear(d_model, rank)
        self.non_linear_func = nn.SiLU()
        self.up_proj = nn.Linear(rank, d_model)

        self.dy_scale = nn.Linear(d_model, 1)
        self.relu = nn.ReLU()

    def forward(self, x, cond):
        # Dy-Scale
        self.scale = self.relu(self.dy_scale(x))
        # Modulate
        x = x + cond
        # Common Adapter Processing
        down = self.down_proj(x)
        down = self.non_linear_func(down)
        up = self.up_proj(down)
        # Update
        output = up * self.scale
        return output

```

2) We insert a modulation layer \mathcal{M} before the down-projection phase to seamlessly infuse task-specific conditions X (z_s or z_{id}) into the adapter module. Striking a balance between performance and parameter efficiency, this modulation is elegantly achieved through the use of addition alone:

$$\mathcal{M}(h) = x + h. \quad (14)$$

3) These adapters are inserted at the multi-head attention (MHA) and feed-forward network (FFN) in a parallel manner, which preserves original features via a separate branch while aggregating updated context through element-wise scaling. Overall,

$$X\text{-Adapter}(h) = s_d \times W_{up} \times \delta(W_{down}\mathcal{M}(h)) + h, \quad (15)$$

where $\delta(\cdot)$ is a SiLU activation in our model. In the fine-tuning process, we selectively update only the newly introduced parameters (orange blocks in Fig. 2(b)), leaving the rest (blue blocks) unchanged.

3.4 Conditional Editing based on x-Adapter

Current holistic methods [2], [3] train on all emotional data under a fixed identity to achieve diverse outputs, but this approach sacrifices the capability for editing. In conjunction with identity- and emotion-agnostic audio processing in Sec. 3.2, the X-Adapter supplements extra conditions during training, thus facilitating further editing during inference. In the following, we describe how to embed emotion and identity information from external sources into latent codes, obtaining z_e and z_{id} .

Emotion Condition. Inspired by GestureDiffuCLIP [39], we aim to align emotion cues to the CLIP domain [13], and enable the use of various multi-modal prompts to indicate emotions. As a result, any accessible modality can serve as guidance, making the application more flexible. Additionally, it can support unknown emotion guidance, thanks to the rich semantics provided by CLIP. As shown in Fig. 3, our system allows users to describe the desired emotion by text, image, audio, and motion sequence. Specifically, for the text prompt, we can directly specify emotional conditions, e.g., The person is happy or provide descriptive prompts for GPT to generate the corresponding emotional text prompts,

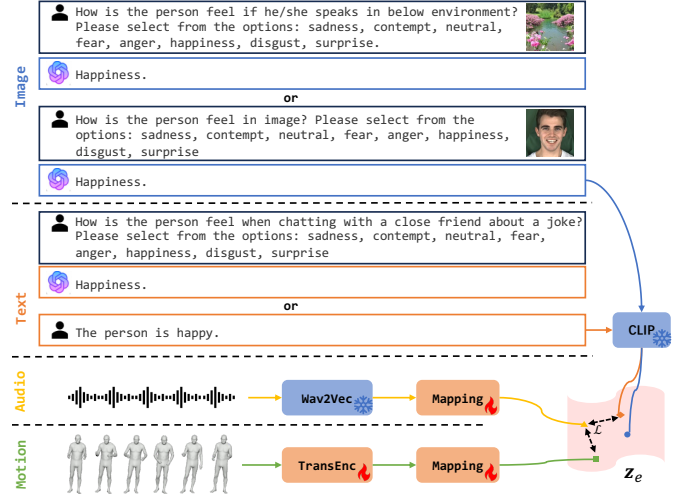


Fig. 3. Overview of multi-modal emotion space within the CLIP domain. In this space, text and image benefit from train-free GPT and CLIP, while audio and motion undergo training to align latent representations with corresponding emotional text embeddings in CLIP space. That is, the emotion cues extracted from a happy audio and happy motion sequence are supervised by the embedding of emotional text prompt The person is happy.

e.g., How is the person feel when chatting with a close friend about a joke, and then extract corresponding embeddings by CLIP encoder. Similarly, we align image prompts with the emotional text prompts by GPT. For example, How is the person feel [a picture of a happy face] or How is the person feel if he/she speaks in [a picture of a beautiful garden]. The above two are train-free. When querying, we instruct GPT to select the most fitting emotional category from the following options [sadness, contempt, neutral, fear, anger, happiness, disgust, surprise]. For the last two, we employ a pretrained wav2vec2.0 [63] model, specialized in emotion recognition, to distill effective information from audio. In parallel, we adopt the framework of Motionclip [67] to learn emotional features from motion sequences. These output cues are further mapped into the CLIP domain and constrained by computing cosine similarity with the CLIP embeddings of emotional text prompts. The above two are trained in BEAT2 [5] dataset. Consequently, our training uses only the embedding derived from text, yet inference allows various modalities as guidance.

Identity Condition. Identity is a crucial factor that affects long-term face and body movements. For example, in BEAT2 dataset [5], Scott is typically quite excited and speaks with broad facial and body gestures, while Nidal tends to be solemn, using only subtle hand movements when speaking. According to the work [68], the identity is closely related to the variance of facial and gesture movements inside each video, we can calculate standard derivation $\sigma(\cdot)$ with respect to frame k of $(F(k), B(k), \frac{\partial F(k)}{\partial k}, \frac{\partial B(k)}{\partial k})$. Formally, given arbitrary video with the reconstructed parameters series $F(k), B(k)$, the identity codes z_{id}^F and z_{id}^B are defined as:

$$z_{id}^F = \text{MLP}([\sigma(F(k)), \sigma(\frac{\partial F(k)}{\partial k})]), \quad (16)$$

$$z_{id}^B = \text{MLP}([\sigma(B(k)), \sigma(\frac{\partial B(k)}{\partial k})]), \quad (17)$$

where MLP performs dimensional mapping, which is trained

along with adapters. Given some video data of a particular identity, we select a clip to calculate the style codes, which are shared for all inputs across subsequent training and testing.

4 EXPERIMENTS

4.1 Experimental Setup

4.1.1 Datasets

BEAT2 is proposed in EMAGE [3], which is built on the original BEAT dataset [5] (containing 76 hours of data for 30 speakers). In particular, BEAT2 transfers the complex annotation of the latter to the standard mesh representation, along with paired audio and text transcripts. We employ the BEAT2-standard portion and adopt 85%, 7.5%, and 7.5% for each identity. In the following experiments, we utilize four identities, Speaker-1 (Wayne), Speaker-2 (Scott), Speaker-11 (Nidal), and Speaker-23 (Hailing).

SHOW [1] is a high-quality audio-visual dataset, which consists of 26.9 hours of in-the-wild talkshow videos from 4 speakers with 3D body meshes at 30fps, and their synchronized audio at a 22K sample rate. We select video sequences longer than 10 seconds and divide the dataset into 80%, 10%, and 10% as train, validation, and test splits.

4.1.2 Implementation Details

We implement our network using PyTorch. The basic DU-Trans contains seven encoder layers and one decoder layer. The hidden dimension of all transformer layers is 512. The bottleneck dimension of X-Adapter is set to 128. Our diffusion model employs a cosine noise schedule, with diffusion steps set to 1000 for training and inference. During pretraining, the learning rate is set to $1e-4$ using the ADAM optimizer with $[\beta_1, \beta_2] = [0.9, 0.99]$ and adjusted to $1e-3$ for fine-tuning experiments. The batch size is consistently set to 128. We train our pretraining model on a single NVIDIA A100 GPU for one day, completing 100,000 iterations. For fine-tuning, we perform 5,000 iterations within one hour. The length of the input motion sequences is 600.

4.1.3 Metrics

We assess the quality of the generated motion from three aspects. For the whole body, we utilize **FMD** [2] to measure the difference between the distributions of the generated holistic motion and ground truth in feature space. It can indicate the overall quality of the holistic motions and the coordination among different body parts. For body gestures, we use **FGD** [69] to measure the distribution difference between generated gesture and ground truth. **BC** [70] quantifies the alignment between the rhythm of the generated gesture and the beat of the audio. **DIV** [36] is a metric for measuring the variations of the synthesized gesture. For face expression, we employ two reconstruction metrics. The vertex **MSE** [28] is calculated to determine the positional distance, and the vertex L1 difference **LVD** [1] is used to assess the discrepancy between the ground truth and the generated facial vertices. Besides, since this task lacks clear ground, human objective evaluation is another main criterion in our method. We conduct an extensive user study to rate the generated motions by different methods in terms of coordination, coherence, and synchronization.

TABLE 1. **Quantitative comparison with SOTA methods on BEAT2 dataset.** The "↓" means the lower, the better, and vice versa. **Bold** and underline represent optimal and suboptimal results. The * indicates training from scratch (pretraining), while the † signifies fine-tuning the emotional model from the neutral pre-trained one. For simplicity, we report $MSE \times 10^{-8}$ and $LVD \times 10^{-5}$ as EMAGE.

Dataset	Method	FMD↓	FGD↓	BC↑	DIV↑	MSE↓	LVD↓
BEAT2 (Scott)	FaceFormer [21]	-	-	-	-	7.725	7.619
	CodeTalker [28]	-	-	-	-	8.133	7.764
	CaMN [5]	1.546	0.668	0.6712	10.36	-	-
	DSG [37]	1.677	0.891	0.7396	<u>10.93</u>	-	-
	Habibie <i>et al.</i> [35]	1.896	0.902	0.7842	8.669	8.658	8.102
	TalkSHOW [1]	1.321	0.871	0.7776	10.42	<u>7.476</u>	7.765
	EMAGE [3]	<u>1.287</u>	<u>0.662</u>	<u>0.7907</u>	13.01	7.703	<u>7.460</u>
	Ours*	1.098	0.563	0.8023	10.48	5.098	6.005
	FaceFormer [21]	-	-	-	-	7.814	7.657
	CodeTalker [28]	-	-	-	-	8.001	7.830
Emotional	CaMN [5]	1.594	0.657	0.6812	10.90	-	-
	DSG [37]	1.640	0.885	0.7405	<u>11.05</u>	-	-
	Habibie <i>et al.</i> [35]	1.903	0.910	0.7797	8.761	8.698	8.143
	TalkSHOW [1]	1.310	0.858	0.7622	10.47	<u>7.531</u>	7.612
	EMAGE [3]	<u>1.239</u>	<u>0.656</u>	<u>0.7990</u>	13.09	7.723	<u>7.471</u>
	Ours†	1.128	0.568	0.8003	10.63	5.015	6.408

4.1.4 Baselines

For BEAT2 dataset [3], we compare our method with representative SOTA approaches in talking head generation: FaceFormer [21] and CodeTalker [28], both of which are tailored for speech-driven 3D facial animation. Additionally, we evaluate against body gesture generation methods, CaMN [5] which introduce the BEAT dataset constructed by using a commercial motion capture system, and DSG [37], a novel diffusion-based co-speech generation method. We reproduce their results in the standardized format of BEAT2 for the face and body respectively. Furthermore, we incorporate assessments of three recent holistic pipelines: the Habibie *et al.* [35] and TalkSHOW [1] are retrained in standardized format either, and EMAGE [3] which directly uses their officially released weights for evaluation. On the SHOW dataset [1], all methods require retraining, including TalkSHOW, as its official weights are general across all identities, whereas other comparison methods like EMAGE are trained for single identity only. To ensure a fair comparison, we retrain TalkShow for each identity. We do not include DiffSHEG [2] and ProbTalk [4] in our comparison since we failed to obtain correct results based on their released codes when retraining them. A more detailed comparison with them will be provided later once the issues are resolved.

4.2 Verification on DU-Trans

4.2.1 Quantitative Results

We first consider a clear training set, Neutral video clips of Scott from BEAT2. We show that our method, trained from scratch (indicated by *), can achieve superior performance than the competing methods. As shown in the top part of Tab. 1, we begin by analyzing the synchronization of facial expressions, our method significantly outperforms the baselines in both MSE and LVD by a large margin, applicable to both specialized talking head generation methods [21], [28] and other holistic motion generation methods [1], [3], [41]. Then, we shift our focus to the quality of gestures, where previous co-speech methods [5], [37] struggle

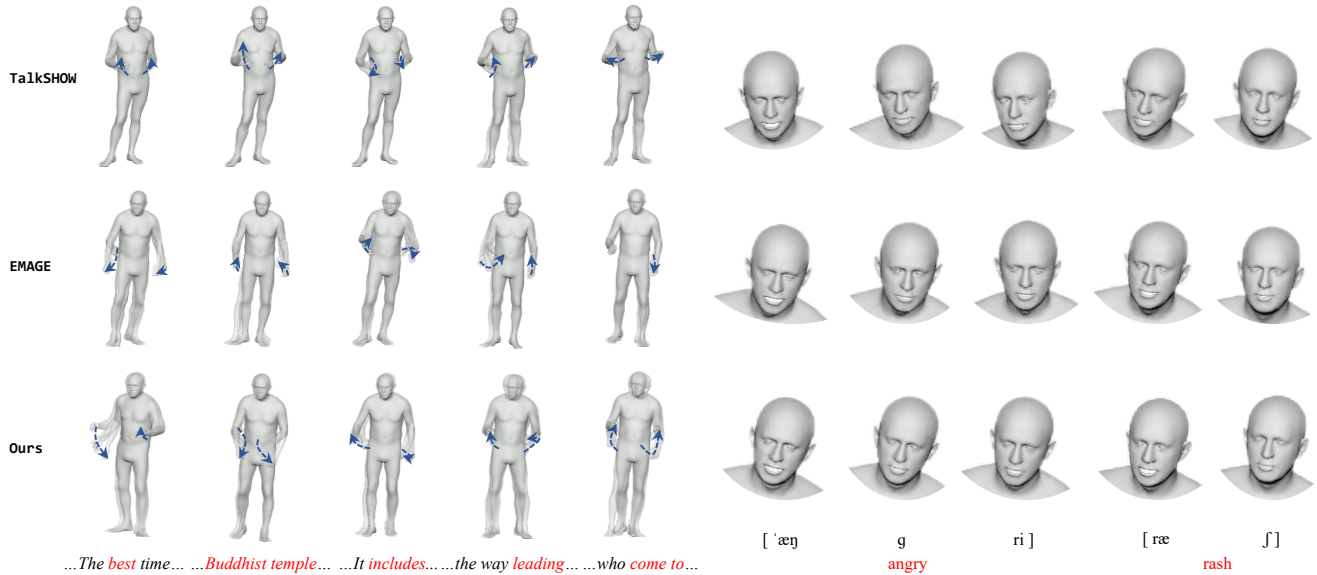


Fig. 4. **Qualitative comparison with TalkSHOW and EMAGE on BEAT2 dataset.** The left part shows the holistic motions while the right presents a close-up of the expressions. Our method can generate expressions and gestures that are synchronized with the audio, particularly producing accurate and diverse gestures for rhythm, semantics, and specific concepts.

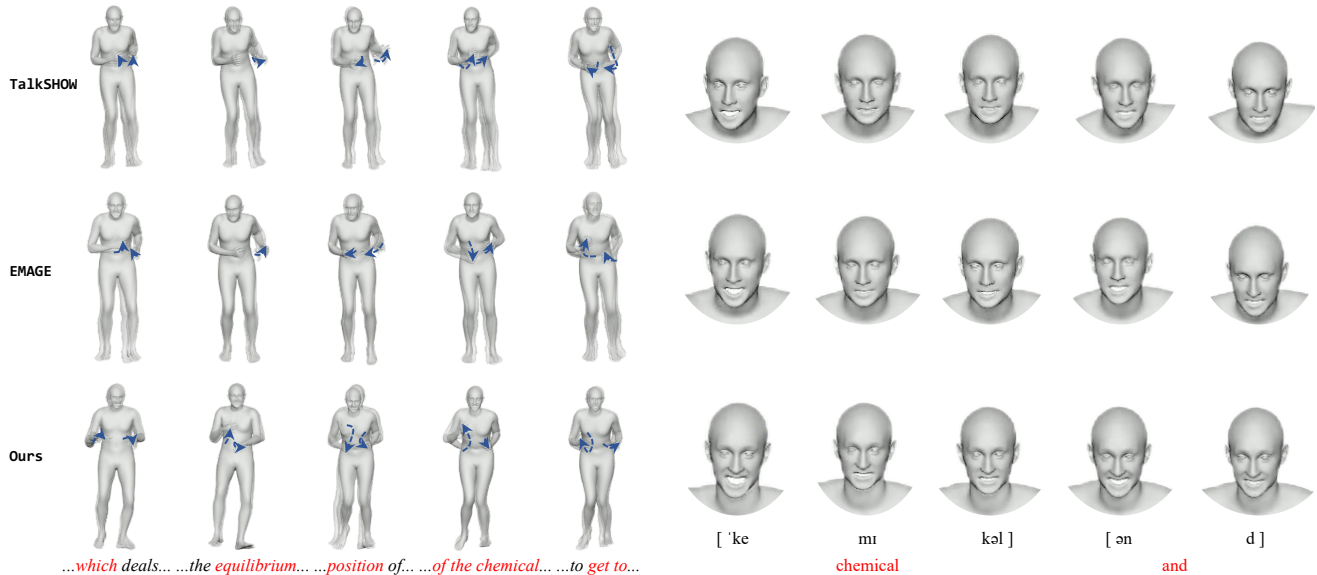


Fig. 5. **Qualitative Comparison with TalkSHOW and EMAGE on SHOW Dataset.** At the left part, we visualize the lower body for all methods.

to match our results. Moreover, our method also outperforms TalkSHOW and EMAGE in terms of FGD and BC, with FGD being particularly notable, which indicates that the distribution of our results is the closest to the ground truth. Note that our method’s DIV metric is slightly lower than that of TalkSHOW and EMAGE, which can be attributed to the fact that the comparative methods include some sudden and exaggerated meaningless movements, leading to a higher score. Finally, we evaluate the motion produced by holistic methods from an comprehensive viewpoint. Our approach shows remarkable advancements in FMD, indicating that it excels in generating synchronized and coordinated holistic body motions. Overall, thanks to the divide and unite mechanism in DU-Trans, our method not only demonstrates superior performance in the metrics of individual components but also clearly leads to holistic metrics. Similar observations could also be concluded

from the quantitative results on SHOW dataset, as shown in Tab. 2. Notably, the solid pre-training performance brought by this powerful basic architecture will benefit the subsequent fine-tuning stage. For more details, please refer to Sec. 4.3.

4.2.2 Qualitative Results

We refer readers to our project website [Combo](#) to for more comprehensive video demonstrations. In this section, we focus qualitative comparison with two recent SOTA methods, TalkSHOW and EMAGE, which can generate coherent motions. While the previous approaches like Habibie *et al.* suffer from varying degrees of jittering, thus we do not include them in this comparison.

On the BEAT2 dataset, we focus on the Scott-Neutral part. As depicted in Fig. 4, TalkSHOW typically displays much slower and less varied motion than the other two, regardless of how the rhythm and semantic content of the audio change. EMAGE, as an

TABLE 2. **Quantitative comparison with SOTA methods on SHOW dataset.** The * indicates training from scratch (pretraining).

Dataset	Method	FMD↓	FGD↓	BC↑	DIV↑	MSE↓	LVD↓
SHOW	FaceFormer [21]	-	-	-	-	137.7	43.86
	CodeTalker [28]	-	-	-	-	140.2	45.54
	CaMN [5]	3.365	2.199	0.7998	10.13	-	-
	DSG [37]	3.462	2.404	0.8295	10.04	-	-
	Habibie <i>et al.</i> [35]	3.851	2.679	0.8510	8.055	145.1	47.11
	TalkSHOW [1]	3.478	2.462	0.8449	10.29	139.3	44.81
	EMAGE [3]	<u>3.380</u>	<u>2.255</u>	<u>0.8585</u>	12.40	<u>136.4</u>	<u>42.74</u>
	Ours*	3.142	2.067	0.8667	<u>10.36</u>	133.5	38.21

improved version of TalkSHOW, utilizes a more comprehensive VQ-VAE to encode the full body and also meticulously upgrades the motion generation network, resulting in superior performance compared to the former. For example, EMAGE can respond to certain words that serve as emphasis, such as "best" and "leading". Yet, it still fails to generate expressive and lifelike gestures. In contrast, our method is not only effective in conveying some concepts such as "Buddhist temple" but also in interpreting semantic words like "includes" and "come to", while being synchronized with rhythmic elements and emphasis, such as "best" and "leading". We further attach the facial meshes to evaluate the lip synchronization at the right part. In comparison with other methods, our model produces expressions that are accompanied by more precise lip shapes and more natural facial motions.

On the SHOW dataset [1], the qualitative results are shown in Fig. 5. Undoubtedly, our method excels in other methods mainly in three aspects: semantic and gesture alignment, rhythm and gesture consistency, and content and facial expression synchronization. Additionally, the coordination among various body parts is not easily depicted in Figs. 4 and 5, we further provide evaluation results in subsequent user studies.

4.2.3 User Study

It is widely acknowledged that assessing the quality of generative tasks is inherently subjective. Despite that we have evaluated with multiple quantitative metrics, there remains a significant gap between such and human visual perception. To this end, we conduct a user study to compare our framework with two recent baselines, TalkSHOW and EMAGE.

Specifically, we randomly select 100 synthesized samples of Scott, including various neutral and emotional clips. Then we recruit 100 subjects with diverse backgrounds to select the most preferred motions in terms of the whole-body **coordination**, holistic **coherence**, and **synchronization** of the expression and gesture with the audio for the shuffled visual results. Besides, in order to help the subjects get used to our questionnaire, we discard the answers of the first three samples and append them in the end to allow participants to get used to the task (test on 103 clips and take the last 100 answers). The results are shown in Tab. 3, our generated holistic motions are dominantly preferred on all three metrics over the competing baselines, especially on coordination and synchronization, which aligns with the superior performance observed in FMD, FGD, and MSE as illustrated in the Tab. 1 and Tab. 2. Thus it can be concluded that DU-Trans extracts the distinctive features of both the face and body while enhancing the harmony between them. Overall, our approach is capable of generating more coordinated, coherent, and synchronized motions that humans prefer.

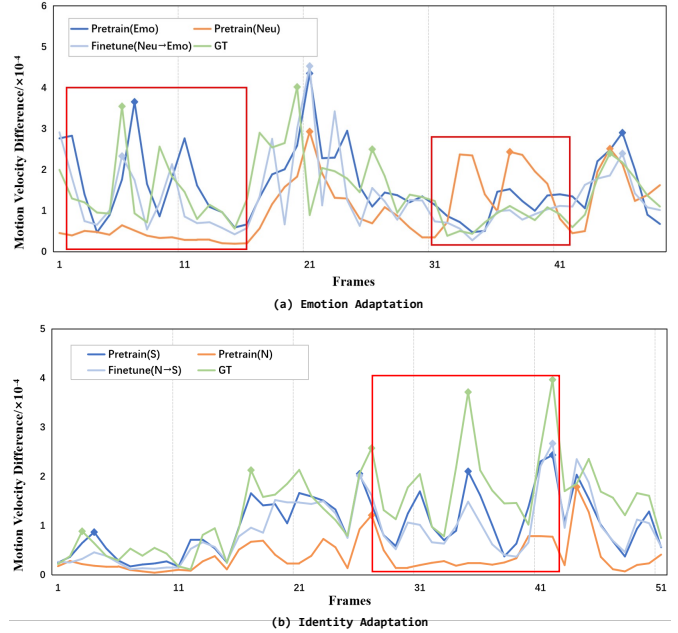


Fig. 6. **Velocity comparisons on BEAT2 of identity and emotion transfer.** Velocity is calculated as the frame-by-frame channel average of the absolute residuals of motion in adjacent frames. These visualizations verify the effectiveness of X-Adapter on sub-task finetuning. Please pay attention to the area highlighted in red rectangular.

TABLE 3. **Results of the user study.** This shows user preference percentage for coordination, coherence, and synchronization. Given that all these methods generate temporally coherent motions, their coherence results are comparably similar. Our methods are mainly preferred for coordination and synchronization.

Method	Coordinated ↑	Coherent ↑	Synchronized ↑
TalkSHOW [1]	0.16	0.30	0.21
EMAGE [3]	0.38	0.34	0.35
Ours	0.46	0.36	0.44

4.3 Verification on x-Adapter

In Sec. 4.3.1, we first analyze the effectiveness of the X-adapter in emotion transfer during training, and then further explore the two benefits it brings: multi-modal editing and unseen emotion editing during inference. These experiments are conducted on Scott data. Then, in Sec. 4.3.2, we analyze the effectiveness of the X-adapter in identity transfer and further validate cross-identity transfer under various conditions. These experiments are conducted on Neutral data. Finally, in Sec. 4.3.3, we provide a detailed analysis of overall tuning efficiency.

4.3.1 Analysis on Emotion Transfer

The Effectiveness of Emotion Transfer. Our proposed X-Adapter enables the transfer from the emotion-agnostic talking body models into the emotional ones, we first give a visualization of motion velocity in Fig. 6(a) to verify the effectiveness of its emotion transfer ability. Specifically, we train two models with our framework: 1) trained with neutral data via DU-Trans; 2) pretrained with neutral data via DU-Trans and then finetuned with emotional data with our X-Adapter. During the test, we randomly sample an emotional clip from the Scott test splits and visualize the velocities of the motions generated by three models, and compare them to the ground truth. We observe that the neutral model outputs a limited dynamic and varied motion, but after fine-tuning, it aligns

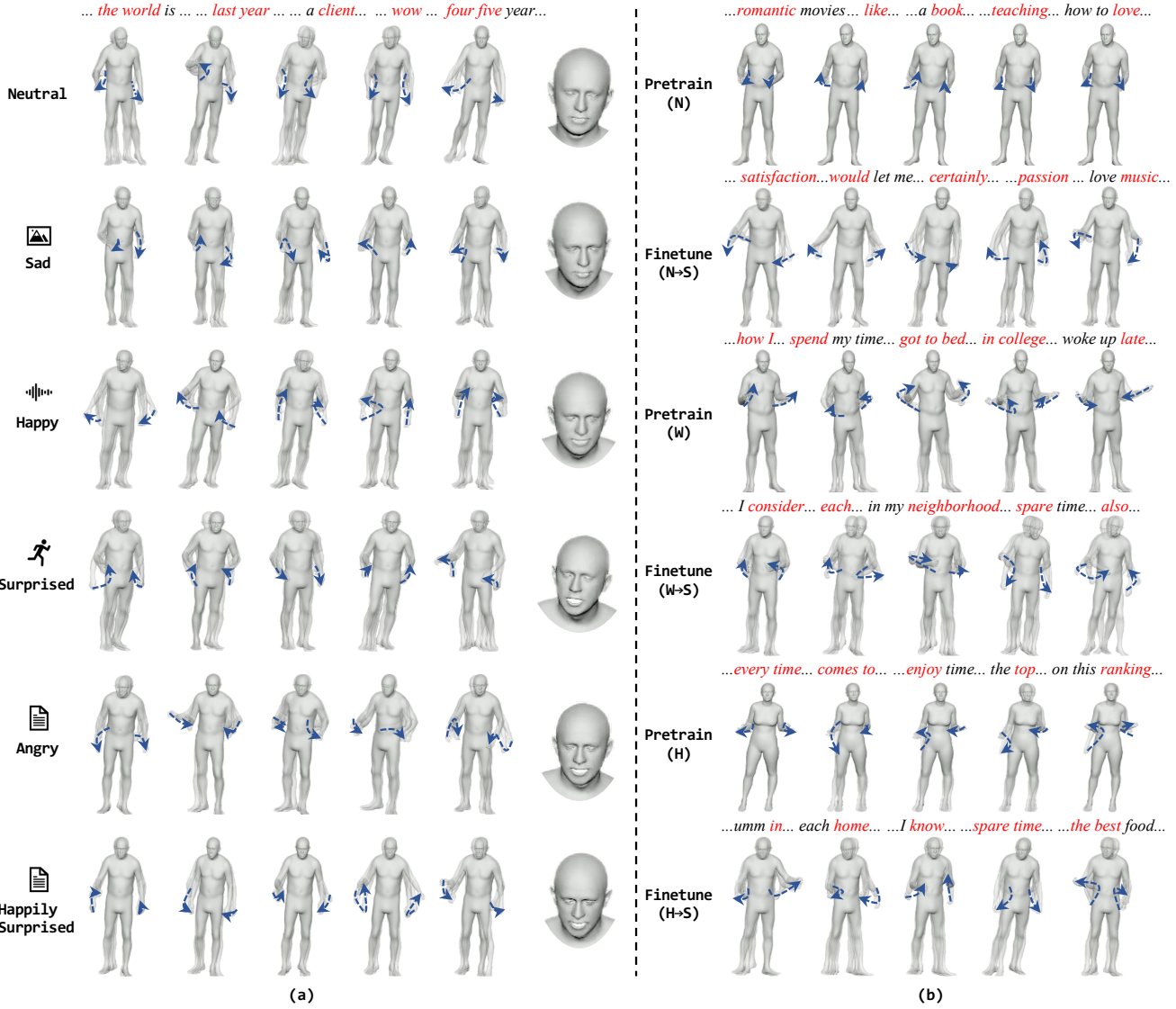


Fig. 7. **The visualization of multi-modal emotion control and different identity personalization.** The left part shows the manipulated outputs guided by sad images, happy audio, surprised motion clips, and angry text. The bottom row is the result of an unseen emotion represented by a happily surprised text prompt. The right part displays the motions from the various source identities as well as the motions after fine-tuning that transfers them to the target identity Scott.

closely with the motion patterns of the ground truth, indicating that the emotion transfer is quite effective. Then, we report the quantitative results in Tab. 4 consistent with the aforementioned conclusions, models from the neutral domain do not perform well on emotional data, as evidenced by their lower performance on all metrics at row Pretrain(Neu), and conversely, after fine-tuning, the performance has seen an overall enhancement as shown in row Finetune(Neu→Emo). To verify the SOTA level of our fine-tuning results, we copy the values of Finetune(Neu→Emo) in Tab. 1 bottom part marked as Ours†. Our method significantly outperforms the baselines on almost all metrics, which is attributed to the solid pretraining performance and excellent cross-domain adaptability.

Additionally, we present the outputs of DU-Trans when fully trained from scratch on emotional data. The results are shown in Fig. 6 at curve Pretrain(emo) and Tab. 4 at row Pretrain(emo), both also exhibit remarkable performance. The comparable results of row Pretrain(emo) and row Finetune(Neu→Emo) indirectly demonstrates the superiority of DU-Trans’s design. However, this

TABLE 4. **Quantitative comparison with several variants of emotion transfer on Scott data.** Emo means emotional while Neu means neutral. The “→” means transferring the pretrained model on source data to the target by fast finetuning. Each row represents the test results of the corresponding method on Scott-Emotional data.

Data	Method	FMD↓	FGD↓	BC↑	DIV↑	MSE↓	LVD↓
Emotional	Pretrain(Neu)	1.749	1.403	0.7810	9.257	5.551	6.880
	Pretrain(Emo)	1.120	0.599	0.8064	11.08	5.149	6.434
	Finetune(Neu→Emo)	1.128	0.568	0.8003	10.63	5.015	6.408

manner lacks flexible editing and adaptability, like the current baselines [1], [2], [3], [4].

Multi-Modal Emotion Editing. As mentioned in Sec. 3.4, our framework allows multi-modal emotion editing. As shown in Fig. 7(a), given neutral audio and multi-modal emotional conditions, we consistently generate gestures that accurately reflect the emotional cues contained in various guidance, including image, audio, motion sequence, and text. For example, our method

produces lowered hand movements that are associated with the sadness depicted in a sad image, *e.g.*, graves, whereas it generates a variety of large gestures with rhythmic body swaying when given a happy audio. Similarly, our method also successfully captures key actions from the surprise motion sequence, such as more frequent body turns and hurried upward gestures. For angry text, it includes more abrupt downward pressing gestures. Additionally, in the fifth column, we display facial meshes at a certain word under different emotions. It is evident that emotions do not interfere with the articulation of speech content, as can be seen from the relatively consistent mouth shapes, but they do influence the overall expression. For instance, when happy, the corners of the mouth turn upwards, and when surprised, the mouth opens wide. Thus, our method allows for precise emotion control of motion generation through any modality, flexibly supporting editing needs in various situations.

Unseen Emotion Editing. In addition to the above, we supplement a qualitative study to demonstrate that the emotion space under the CLIP domain possesses a certain degree of generalization ability, thanks to the rich semantics inherited from CLIP. As shown in Fig. 7(a), row 6 shows the results of the given *happily surprised* in text prompts. This is an unseen compound emotion, and the generated motions accurately convey happiness and surprise simultaneously, which can be observed from the overall lively body movements and astonished expressions. Besides, by comparing the facial details with those of happy (row 3) or surprised (row 4), the result of this unseen style is not a mere replication of either but rather a full combination of both. This experiment verifies the flexibility and rich semantic priors of the CLIP feature space.

4.3.2 Analysis on Identity Transfer

The Effectiveness of Identity Transfer. Similar to Sec. 4.3.1, we perform qualitative and quantitative experiments to verify the effectiveness of X-Adapter in identity transfer. First, we visualize the motion velocity curves for four methods, *i.e.*, ground truth, Scott model, Nidal model, and the Nidal model after finetuned on Scott data, when each receives a randomly sampled Scott audio signal. As shown in Fig. 6(b), Nidal usually speaks in a calm and quiet manner, which corresponds to the motion curve displaying a smooth low-amplitude trajectory, as colored in orange. On the other hand, our fast adaption helps to transfer to the lively and dynamic Scott style, *i.e.*, the light blue curve exhibits similar variations and intensities to the ground truth in green and the Scott model in blue. Second, we attach the quantitative results in Tab. 5 to support the above observations. Concretely, row Pretrain(N) demonstrates that direct cross-identity evaluation does not yield satisfactory results, while slight fine-tuning can achieve competitive performance compared to a model sufficiently trained from scratch, as shown by comparing row Pretrain(S) and row Finetune(N→S).

Cross-Identity Transfer Analysis. To further verify that our method is robust to the choice of source identity and can be transferred to any other identity, we provide a cross-identity transfer analysis. Specifically, we construct three identity pairs with significant gaps: 1) Nidal and Scott have different personalities, one being quiet and the other being lively; 2) Wayne and Scott, although similar in temperament, have different behavioral habits; 3) Hailing and Scott have different genders. As shown in Tab. 5, the rows Pretrain(S), Finetune(N→S), Finetune(W→S), and Finetune(H→S) exhibit a comparable performance, from which we can infer that the above three distinct identities can

TABLE 5. **Quantitative comparison with several variants of identity transfer on neutral data.** S, N, W, and H are the abbreviations for Scott, Nidal, Wayne, and Hailing, respectively. Each row represents the test results of the corresponding method on Scott-Neutral data.

Data	Method	FMD↓	FGD↓	BC↑	DIV↑	MSE↓	LVD↓
	Pretrain(S)	1.098	0.563	0.8023	10.48	5.098	6.005
Scott-Neutral	Pretrain(N)	9.231	2.883	0.0149	0.551	15.20	11.43
	Finetune(N→S)	1.326	0.680	0.7888	9.790	4.926	6.002
	Pretrain(W)	3.955	3.656	0.4379	3.265	8.017	7.507
	Finetune(W→S)	1.223	0.513	0.8083	9.998	5.800	6.431
	Pretrain(H)	7.752	6.488	0.6393	5.691	10.76	9.243
	Finetune(H→S)	1.137	0.480	0.8169	10.02	5.860	6.614

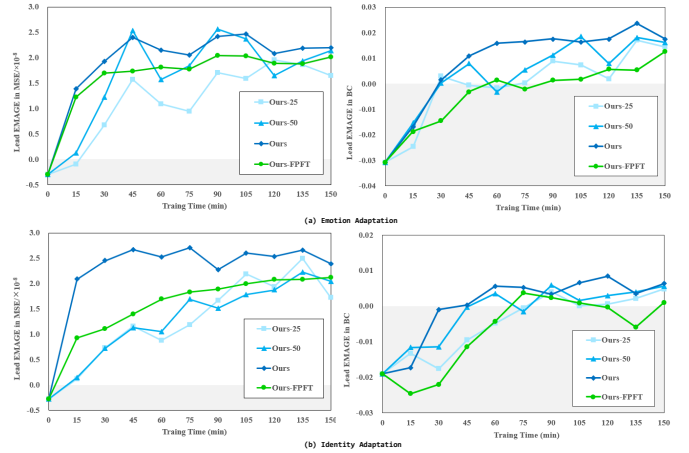


Fig. 8. **Tuning efficiency of X-Adapter.** In this visualization, we choose MSE for the face and BC for the body. Values below 0 on the y-axis (gray fill) indicate inferior performance compared to EMAGE, and vice versa. Our design exhibits exceptional tuning efficiency in terms of training time and data, achieving SOTA performance within 45 minutes with full (Ours) or half data (Ours-50), or even within 90 minutes with only 25% training data (Ours-25). Ours-FPFT means full-parameter finetuning on DU-Trans (w/o. X-adapter) with full data.

all be transferred onto Scott style. Besides, we supplement the intuitive visualizations in Fig. 7(b). In line with the above, each person exhibits their own unique movement dynamics. Nidal (row 1) shows less variety in his movements and changes slowly. Wayne (row 3) is accustomed to swinging his arms and speaking while facing to the left. Hailing (row 5) possesses a characteristically feminine grace. After efficient finetuning (rows 2, 4, 6), our approach successfully adjusts the movement patterns to match Scott’s, no matter the initial state. In conclusion, X-Adapter is capable of handling various challenging identity transfer tasks.

4.3.3 Tuning Efficiency

In this part, we provide a detailed analysis to demonstrate that X-Adapter can efficiently adapt the pretrained DU-Trans of Scott neutral data to alternative identity or emotion, even with limited training data.

Firstly, we emphasize that our finetuning only updates about 4M parameters for both identity and emotion adaptation, in which the adapter is 3.73M and three heads are 0.27 M, while the total number of parameters is around 40M, meaning we only utilize 10% of the trainable parameters yet achieve superior performance.

Secondly, we analyze the efficiency of our finetuning on training *time* and *data*. Specifically, we conduct periodic tests every 15 minutes during the identity and emotion transfer process

(a) Ablation on DU-Trans.								(b) Ablation on X-Adapter.									
	Method	P(M)	FMD↓	FGD↓	BC↑	DIV↑	MSE↓	LVD↓		Method	P(M)	FMD↓	FGD↓	BC↑	DIV↑	MSE↓	LVD↓
Architecture	$l = 0, j = 8$	19.46	1.265	0.635	0.7921	9.972	5.795	6.611	Location	Serial	4.00	1.332	0.595	0.7793	10.58	5.610	6.840
	$l = 8, j = 0$	35.89	1.336	0.588	0.7695	9.350	5.465	6.428		Parallel	4.00	1.128	0.568	0.8003	10.63	5.015	6.408
	$l = 7, j = 1$	34.84	1.190	0.579	0.7999	9.991	5.362	6.358		Only MHA	2.14	1.312	0.581	0.7942	10.63	5.237	6.581
	$l = 5, j = 3$	32.74	1.214	0.580	0.7904	9.895	5.488	6.529		Only FFN	2.14	1.427	0.595	0.7825	10.60	5.282	6.554
	$l = 3, j = 5$	30.64	1.278	0.589	0.7917	9.658	5.602	6.601		Condition	w/o. x	4.00	1.236	0.572	0.7953	10.11	5.329
Loss	w/o. $\mathcal{L}_F, \mathcal{L}_B$	34.84	30.57	27.19	0.8442	32.46	2910	109.3	Stylization		8.14	1.120	0.567	0.8002	10.59	5.228	6.506
	$\lambda_F, \lambda_B = 1$	34.84	1.412	0.593	0.7978	9.963	5.373	6.407	Add		4.00	1.128	0.568	0.8003	10.63	5.015	6.408
	$\lambda_F, \lambda_B = 0.5$	34.84	1.190	0.579	0.7999	9.995	5.362	6.358	Scale	Scalar-1.0	3.99	1.236	0.569	0.7987	9.890	7.044	7.316
	$\lambda_F, \lambda_B = 0.1$	34.84	1.468	0.598	0.7904	9.880	5.671	6.544		L-Scalar	3.99	1.256	0.584	0.8001	10.15	5.464	6.781
Bi-Flow	$l = 1$	36.94	1.198	0.586	0.7927	9.717	5.226	6.299	Dy-Scale	4.00	1.128	0.568	0.8003	10.63	5.015	6.408	
	$l = 3$	36.94	1.098	0.563	0.8023	10.48	5.098	6.005	PEFT	LoRA-r64	2.17	1.205	0.581	0.7911	10.17	5.341	6.659
	$l = 6$	36.94	1.128	0.579	0.8002	9.986	5.212	6.010		Prefix Tuning	0.03	2.234	1.281	0.7673	6.156	7.943	8.063
	$l = 3, 4$	39.05	1.097	0.565	0.8025	10.45	5.111	6.001		Adapter-r64	2.17	1.191	0.578	0.7906	10.37	5.226	6.654
	$l = 2, 3, 4$	41.15	1.105	0.568	0.8020	10.44	5.087	5.997		Adapter-r128	4.00	1.128	0.568	0.8003	10.63	5.015	6.408

TABLE 6. Quantitative ablations for DU-Trans and X-Adapter. The ablation studies of DU-Trans are conducted on the Scott-Neutral in BEAT2 while that of X-Adapter are conducted on the Scott-Emotional.

to evaluate the tuning time and data efficiency and record the MSE metric for face expression and BC metric for body gesture at each time point. Comparing our method to EMAGE, we plot the leading value in Fig. 8. Specifically, our method outperforms SOTA results within 45 minutes with full or half data, and can also achieve the best output with just a quarter of the data within 90 minutes. Notably, we open all parameters of DU-Trans and use full data for finetuning (as shown in green color), but its performance is not as good as parameter-efficient finetuning (as shown in deep blue color), even costing many trainable parameters. Beyond the above, we find that: 1) the time required for facial performance to reach comparable levels is relatively shorter than that for gestures, as expressions only involve a small range of facial movements, whereas gestures encompass a larger scope. For example, just 15 minutes of fine-tuning is sufficient for our method to surpass the SOTA competitor on the MSE metric; 2) in contrast to finetuning with a limited dataset, employing the full dataset can swiftly improve performance in a short period, but as time progresses, it typically saturates at a comparable level in the end. To sum up, users can dynamically adjust the finetuning duration based on the amount of data available.

4.4 Ablation Study

In this part, we ablate on the proposed DU-Trans and X-Adapter to validate our design choices and hyperparameters.

4.4.1 Ablation on DU-Trans

In Tab. 6(a), we conduct the ablation study on DU-Trans from three aspects, *i.e.*, architecture, loss functions, and Bi-Flow variants. The architecture ablation study employs auxiliary losses with optimal weights but does not utilize the Bi-Flow. The loss ablation study fixes the optimal architecture without including the Bi-Flow. Finally, the last study ablates the Bi-Flow on the optimal architecture incorporated with auxiliary losses.

Analysis on Basic Architecture (Tab. 6(a) Architecture part). The insight of our DU-Trans is to use divided encoders to ensure sufficient exhibition for both face and body, followed by a united decoder to implicitly model their interconnections and to directly predict the combined coefficients for overall high coordination. To verify its effectiveness, we first design two variants, the one with

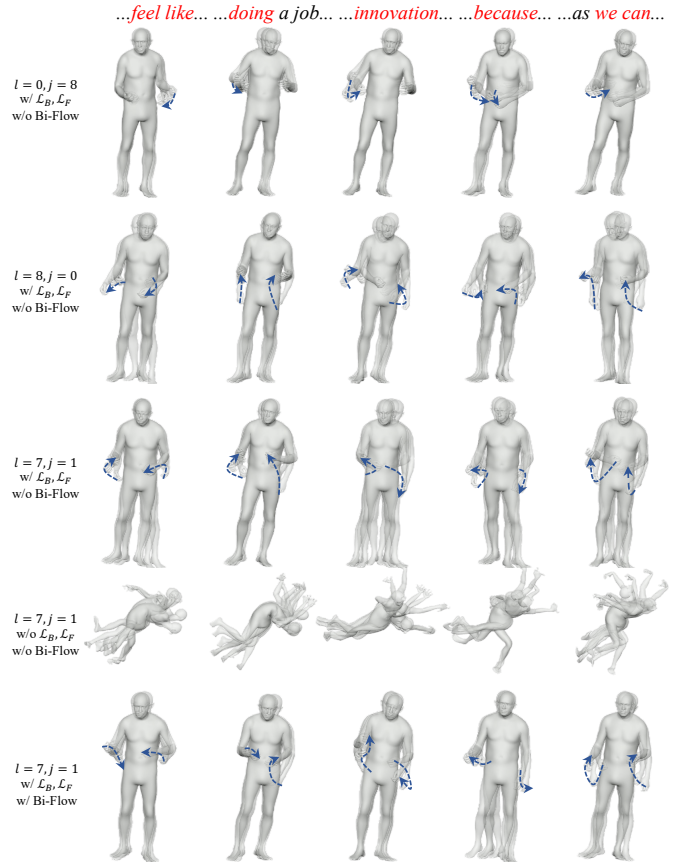


Fig. 9. Qualitative ablations for DU-Trans. The full version of DU-Trans ($l = 7, j = 1, w/\mathcal{L}_B, \mathcal{L}_F, w/\text{Bi-Flow}$) produces shows more synchronized and meaningful motions than other ablations.

only two divided encoders (row $l = 8, j = 0$, where l is the number of encoder layers and j is the number of decoder layers) and the other with only a united decoder (row $l = 0, j = 8$). The results indicate that neither of them yields satisfactory outputs. The underlying reason may be that the two separate encoders do not account for each other's influence, which is evident from the significant degradation in FMD. Directly employing a single decoder may cause two distinct distributions to converge toward each

other, ensuring harmony but greatly sacrificing the uniqueness of each, especially as indicated by the decline in FGD and MSE. We also give a visualization in Fig. 9 that the motion generated by this method has a minimal amplitude. Then, we explore how to preserve individual differences while achieving a harmonious commonality. As shown in row $l = 7, j = 1$, when the encoder has 7 layers and the decoder has 1 layer, our DU-Trans achieves the best performance.

Analysis on Loss Functions (Tab. 6(a) Loss part). The two auxiliary losses for face and body branches are critical to distilling their respective features and aiding in the joint learning of holistic motion. To verify their effectiveness, we present the quantitative results in the Loss part. It is obvious that the absence of auxiliary loss (row w/o. λ_F, λ_B) leads to a significant decrease in most metrics except for BC and DIV. These two are unreliable when there is a noticeable jitter in the motion. This observation can also be discerned in the fourth row in Fig. 9, *i.e.*, exhibiting unreasonable poses and meaningless movements. Furthermore, we explore the optimal hyperparameters for these losses and find that the optimal set is $\lambda_F = \lambda_B = 0.5$.

Analysis on Bi-Flow (Tab. 6(a) Bi-Flow part). The Bi-Flow design is utilized during the divide phase for the face and body to provide global dynamic cues that enhance their respective performances. As shown in the Bi-Flow part, we examine the impact of hyperparameters regarding Bi-Flow, including its position (first 3 rows in this part) and number (the remaining). Concretely, when we apply this module at the shallow layer $l = 1$ and the deep layer $l = 6$, the performance does not match that at the intermediate layer $l = 3$. From row $\lambda_F = \lambda_B = 0.5$ of the Loss part and $l = 3$ of the Bi-Flow part, we observe that models incorporating this bidirectional interaction enhance the performance of both the face and body, particularly the face, which shows particularly significant improvement in all metrics. This is consistent with the operation in EMAGE that uses a unidirectional data flow from body to face, yet we find that the reverse flow can also help learning of the body. Besides, this interacted layer also promotes the coordination of the holistic motion, reflecting on the FMD metric. We also provide a qualitative comparison in Fig. 9 to support the above conclusion. Furthermore, building on the foundation of $l = 3$, we increase the number of Bi-Flow layers. As indicated in rows $l = 3, 4$ and $l = 2, 3, 4$, it is observed that while the metrics do not see a significant improvement, the number of trainable parameters increases substantially, *i.e.*, each this layer causing about 5% parameters. Consequently, we determine that placing a single Bi-Flow module at the third layer provides a better balance between tunable parameters and overall performance.

4.4.2 Ablation on X-Adapter

In this section, we ablate the X-Adapter structure under the emotion transfer task from four aspects, *i.e.*, insert location, condition integration method, scale form, and PEFT variants. The results are summarized in Tab. 6(b), where each row only contains one modification over the full version.

Analysis on Insertion Form and Position (Tab. 6(b) Location part). We explore how to insert the added adapter into the original network by comparing the parallel and sequential instances. As shown in rows Serial and Parallel, the parallel form outperforms the sequential one in all metrics. This could be attributed to the parallel adapter receiving the same input as the sub-layers and directly updating the output, which is a more intuitive and natural design. This approach minimally impacts the original model,

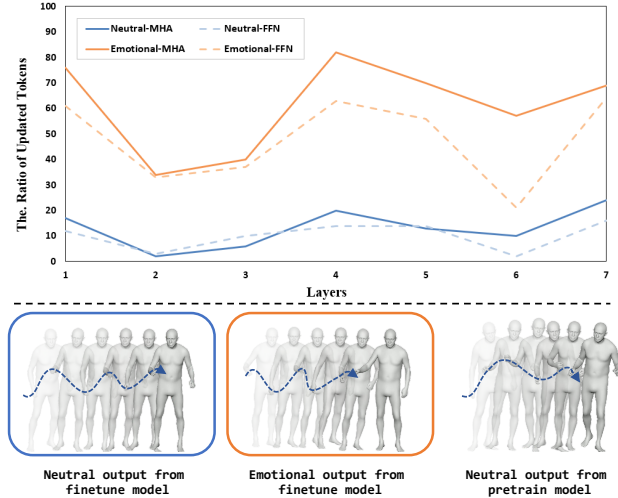


Fig. 10. **Qualitative visualizations for Dy-Scale.** We display the ratio of updated tokens in Dy-Scale for each layer across different inputs (Neutral and Emotional), and the output motions of three variants.

as the adapter operates independently of the sub-layer outputs. Moreover, we attempt to reduce the use of adapters to reduce the number of trainable parameters. However, from rows Only MHA and Only FFN, we observe that fine-tuning only the adapters inserted into either the FFN or MHA leads to a certain degree of performance decline under the same training settings. Thus, we incorporate our X-Adapter for *both* the FFN and MHA.

Analysis on Condition (Tab. 6(b) Condition part). It is essential to incorporate the corresponding conditions to control the fine-tuning of emotions or identities. As shown in this part, when the injection of conditions is removed (row w/o. X), all metrics exhibit degradation, indicating that conditions can guide the network to better express the desired information. Moreover, the absence of conditions can also lead to a loss of editing capabilities during the inference phase. We further explore how to integrate the conditions. An intuitive approach is to use a stylization method [71], mapping the conditions into the scale and shift factors to affect the original features, as shown in row Stylization. Although introducing this module enhances performance, it significantly increases the number of trainable parameters, *i.e.*, from 4M to 8.14M. To balance the performance and cost, we continue to experiment with an extreme case, directly adding the condition to the original features without adding any trainable parameters. To our delight, we find that this simple method can achieve comparable results. Therefore, we employ the addition manner to exert the influence of conditions.

Analysis on Scale Form (Tab. 6(b) Scale part). We introduce a dynamic scale mechanism (Dy-Scale) in X-Adapter to dynamically adjust the original features by considering the significance score of the tunable features. To verify its effectiveness, we conduct experiments on two ablated variations: the fixed scalar scale which is set to 1.0 (row Scalar-1.0), and the learnable scalar scale which is initialized by 1.0 (row L-Scalar). As shown in this part, our Dy-Scale yields the best performance with a negligible increase in tunable parameters, from 3.99M to 4.00M. Thus, for such complex temporal motions, learning an adaptive weight for each frame is an intuitive and effective strategy. We further visualize the ratio of updated tokens in each layer for both MHA and FFN to explore the mechanism of Dy-Scale. As shown in Fig. 10, the *same* audio input exhibits similar changes across different layers

of MHA and FFN under various emotional conditions, but the specific ratios are entirely distinct. The neutral output from the fine-tuned model has only a few activated tokens because it shares similar motion patterns as the neutral output from the pre-trained model. In contrast, the emotional output is entirely different, which can also be discerned from the adjustment ratio.

Analysis on Other PEFT Methods (Tab. 6(b) PEFT part).

To further prove the effectiveness of our proposed X-Adapter, we compare it with several PEFT approaches, *i.e.*, Prefix Tuning [45] and LoRA [47], under the same training time and data. Specifically, prefix tuning involves prepending 64 learnable tokens in the temporal dimension and adding the conditions to them. From row Prefix Tuning, it is evident that this manner does not achieve effective transfer. While the number of trainable parameters is minimal, it cannot be ignored that an increase in the number of tokens also leads to a substantial increase in memory consumption. Besides, to ensure a fair comparison, we adapt Dy-Scale and the condition in the same manner as LoRA. We set the rank r for both to be 64 thus the tunable parameters are the same. By comparing rows LoRA-r64 and Adapter-r64, the overall performance of the X-Adapter is superior to that of LoRA. Furthermore, we attempt to increase the rank to 128. As observed in rows Adapter-r128 and Adapter-r64, while the number of trainable parameters has increased, there is a noticeable improvement in overall performance. The potential reason may be that complex motion patterns require more parameters to be well-fitted during the fine-tuning phase. Experimentally, we employ the proposed X-Adapter with rank set to 128 in the full version.

5 CONCLUSION

In this work, we focus on enhancing the user experience with talking avatars, concentrating on the harmony of full-body movements and the rapid adaptation of new identity and emotional data. To achieve such, we propose `Combo`, which includes two critical designs: 1) DU-Trans operates by initially dividing into dual pathways designed to independently learn the distinct features of the face and body, each guided by auxiliary losses and enriched with holistic dynamic priors through the Bi-Flow layer. Then, it unites the learned two features to model a joint distribution and directly predicts the combined coefficients that ensure a high degree of coordinated holistic motions. 2) X-Adapter seamlessly integrates into a pretrained DU-Trans network that can quickly transfer the original model to an emotional one or other totally different identities with much fewer trainable parameters. Our approach has demonstrated state-of-the-art performance on two public datasets, along with an efficient ability to transfer identities and emotions.

Limitations: Despite the significant improvements, `Combo` still suffers from several limitations. First, since we do not perform targeted design for the foot trajectory, the motion generated by our method exhibits physical implausibilities of foot sliding. We plan to introduce explicit physical modeling to mitigate this issue. Second, due to the limitations of BEAT2 and SHOW datasets, we are unable to generate highly photo-realistic avatars, which is crucial for enhancing the user experience. We aim to develop a large-scale multi-view full-body talking avatar dataset to prompt the advancement of this field.

REFERENCES

[1] H. Yi, H. Liang, Y. Liu, Q. Cao, Y. Wen, T. Bolkart, D. Tao, and M. J. Black, "Generating holistic 3d human motion from speech," in

Proceedings of the IEEE/CVF Conference on Computer Vision and Pattern Recognition, 2023, pp. 469–480.

[2] J. Chen, Y. Liu, J. Wang, A. Zeng, Y. Li, and Q. Chen, "Diffshg: A diffusion-based approach for real-time speech-driven holistic 3d expression and gesture generation," *arXiv preprint arXiv:2401.04747*, 2024.

[3] H. Liu, Z. Zhu, G. Becherini, Y. Peng, M. Su, Y. Zhou, N. Iwamoto, B. Zheng, and M. J. Black, "Emage: Towards unified holistic co-speech gesture generation via masked audio gesture modeling," *arXiv preprint arXiv:2401.00374*, 2023.

[4] Y. Liu, Q. Cao, Y. Wen, H. Jiang, and C. Ding, "Towards variable and coordinated holistic co-speech motion generation," *arXiv preprint arXiv:2404.00368*, 2024.

[5] H. Liu, Z. Zhu, N. Iwamoto, Y. Peng, Z. Li, Y. Zhou, E. Bozkurt, and B. Zheng, "Beat: A large-scale semantic and emotional multi-modal dataset for conversational gestures synthesis," in *European conference on computer vision*. Springer, 2022, pp. 612–630.

[6] X. Chen, L. Huang, Y. Liu, Y. Shen, D. Zhao, and H. Zhao, "Anydoor: Zero-shot object-level image customization," in *Proceedings of the IEEE/CVF Conference on Computer Vision and Pattern Recognition*, 2024, pp. 6593–6602.

[7] Z. Li, M. Cao, X. Wang, Z. Qi, M.-M. Cheng, and Y. Shan, "Photomaker: Customizing realistic human photos via stacked id embedding," in *Proceedings of the IEEE/CVF Conference on Computer Vision and Pattern Recognition*, 2024, pp. 8640–8650.

[8] Z. Xu, J. Zhang, J. H. Liew, J. Feng, and M. Z. Shou, "Xagen: 3d expressive human avatars generation," *Advances in Neural Information Processing Systems*, vol. 36, 2024.

[9] X. Peng, J. Zhu, B. Jiang, Y. Tai, D. Luo, J. Zhang, W. Lin, T. Jin, C. Wang, and R. Ji, "Portraitbooth: A versatile portrait model for fast identity-preserved personalization," in *Proceedings of the IEEE/CVF Conference on Computer Vision and Pattern Recognition*, 2024, pp. 27 080–27 090.

[10] L. Yin, Y. Wang, T. He, J. Liu, W. Zhao, B. Li, X. Jin, and J. Lin, "Emog: Synthesizing emotive co-speech 3d gesture with diffusion model," *arXiv preprint arXiv:2306.11496*, 2023.

[11] X. Qi, C. Liu, L. Li, J. Hou, H. Xin, and X. Yu, "Emotiongesture: Audio-driven diverse emotional co-speech 3d gesture generation," *arXiv preprint arXiv:2305.18891*, 2023.

[12] Z. Han, C. Gao, J. Liu, S. Q. Zhang *et al.*, "Parameter-efficient fine-tuning for large models: A comprehensive survey," *arXiv preprint arXiv:2403.14608*, 2024.

[13] A. Radford, J. W. Kim, C. Hallacy, A. Ramesh, G. Goh, S. Agarwal, G. Sastry, A. Askell, P. Mishkin, J. Clark *et al.*, "Learning transferable visual models from natural language supervision," in *International conference on machine learning*. PMLR, 2021, pp. 8748–8763.

[14] G. Pavlakos, V. Choutas, N. Ghorbani, T. Bolkart, A. A. Osman, D. Tzionas, and M. J. Black, "Expressive body capture: 3d hands, face, and body from a single image," in *Proceedings of the IEEE/CVF conference on computer vision and pattern recognition*, 2019, pp. 10 975–10 985.

[15] E. Ng, J. Romero, T. Bagautdinov, S. Bai, T. Darrell, A. Kanazawa, and A. Richard, "From audio to photoreal embodiment: Synthesizing humans in conversations," *arXiv preprint arXiv:2401.01885*, 2024.

[16] M. H. Mughal, R. Dabral, I. Habibie, L. Donatelli, M. Habermann, and C. Theobalt, "Convofusion: Multi-modal conversational diffusion for co-speech gesture synthesis," *arXiv preprint arXiv:2403.17936*, 2024.

[17] S. Shen, W. Zhao, Z. Meng, W. Li, Z. Zhu, J. Zhou, and J. Lu, "Difftalk: Crafting diffusion models for generalized audio-driven portraits animation," in *Proceedings of the IEEE/CVF Conference on Computer Vision and Pattern Recognition*, 2023, pp. 1982–1991.

[18] C. Xu, J. Zhu, J. Zhang, Y. Han, W. Chu, Y. Tai, C. Wang, Z. Xie, and Y. Liu, "High-fidelity generalized emotional talking face generation with multi-modal emotion space learning," in *Proceedings of the IEEE/CVF conference on computer vision and pattern recognition*, 2023, pp. 6609–6619.

[19] C. Xu, S. Zhu, J. Zhu, T. Huang, J. Zhang, Y. Tai, and Y. Liu, "Multimodal-driven talking face generation via a unified diffusion-based generator," *arXiv preprint arXiv:2305.02594*, 2023.

[20] Z. Peng, H. Wu, Z. Song, H. Xu, X. Zhu, J. He, H. Liu, and Z. Fan, "Emotalk: Speech-driven emotional disentanglement for 3d face animation," in *Proceedings of the IEEE/CVF International Conference on Computer Vision*, 2023, pp. 20 687–20 697.

[21] Y. Fan, Z. Lin, J. Saito, W. Wang, and T. Komura, "Faceformer: Speech-driven 3d facial animation with transformers," in *Proceedings of the IEEE/CVF Conference on Computer Vision and Pattern Recognition*, 2022, pp. 18 770–18 780.

- [22] M. Villanueva Aylagas, H. Anadon Leon, M. Teye, and K. Tollmar, "Voice2face: Audio-driven facial and tongue rig animations with cvaeas," in *Computer Graphics Forum*, vol. 41, no. 8. Wiley Online Library, 2022, pp. 255–265.
- [23] C. Zhang, S. Ni, Z. Fan, H. Li, M. Zeng, M. Budagavi, and X. Guo, "3d talking face with personalized pose dynamics," *IEEE Transactions on Visualization and Computer Graphics*, vol. 29, no. 2, pp. 1438–1449, 2021.
- [24] D. Cudeiro, T. Bolkart, C. Laidlaw, A. Ranjan, and M. J. Black, "Capture, learning, and synthesis of 3d speaking styles," in *Proceedings of the IEEE/CVF conference on computer vision and pattern recognition*, 2019, pp. 10 101–10 111.
- [25] Z. Peng, Y. Luo, Y. Shi, H. Xu, X. Zhu, H. Liu, J. He, and Z. Fan, "Self-talk: A self-supervised commutative training diagram to comprehend 3d talking faces," in *Proceedings of the 31st ACM International Conference on Multimedia*, 2023, pp. 5292–5301.
- [26] A. Van Den Oord, O. Vinyals *et al.*, "Neural discrete representation learning," *Advances in neural information processing systems*, vol. 30, 2017.
- [27] E. Ng, H. Joo, L. Hu, H. Li, T. Darrell, A. Kanazawa, and S. Ginosar, "Learning to listen: Modeling non-deterministic dyadic facial motion," in *Proceedings of the IEEE/CVF Conference on Computer Vision and Pattern Recognition*, 2022, pp. 20 395–20 405.
- [28] J. Xing, M. Xia, Y. Zhang, X. Cun, J. Wang, and T.-T. Wong, "Codetalker: Speech-driven 3d facial animation with discrete motion prior," in *Proceedings of the IEEE/CVF Conference on Computer Vision and Pattern Recognition*, 2023, pp. 12 780–12 790.
- [29] J. Ho, A. Jain, and P. Abbeel, "Denoising diffusion probabilistic models," *Advances in neural information processing systems*, vol. 33, pp. 6840–6851, 2020.
- [30] S. Aneja, J. Thies, A. Dai, and M. Nießner, "Facetalk: Audio-driven motion diffusion for neural parametric head models," *arXiv preprint arXiv:2312.08459*, 2023.
- [31] P. Chen, X. Wei, M. Lu, Y. Zhu, N. Yao, X. Xiao, and H. Chen, "Diffusiotalker: Personalization and acceleration for speech-driven 3d face diffuser," *arXiv preprint arXiv:2311.16565*, 2023.
- [32] S. Stan, K. I. Haque, and Z. Yumak, "Facediffuser: Speech-driven 3d facial animation synthesis using diffusion," in *Proceedings of the 16th ACM SIGGRAPH Conference on Motion, Interaction and Games*, 2023, pp. 1–11.
- [33] Z. Sun, T. Lv, S. Ye, M. G. Lin, J. Sheng, Y.-H. Wen, M. Yu, and Y.-j. Liu, "Diffposotalk: Speech-driven stylistic 3d facial animation and head pose generation via diffusion models," *arXiv preprint arXiv:2310.00434*, 2023.
- [34] B. Thambiraja, S. Aliakbarian, D. Cosker, and J. Thies, "3diface: Diffusion-based speech-driven 3d facial animation and editing," *arXiv preprint arXiv:2312.00870*, 2023.
- [35] C. Ahuja, D. W. Lee, Y. I. Nakano, and L.-P. Morency, "Style transfer for co-speech gesture animation: A multi-speaker conditional-mixture approach," in *Computer Vision—ECCV 2020: 16th European Conference, Glasgow, UK, August 23–28, 2020, Proceedings, Part XVIII 16*. Springer, 2020, pp. 248–265.
- [36] J. Li, D. Kang, W. Pei, X. Zhe, Y. Zhang, Z. He, and L. Bao, "Audio2gestures: Generating diverse gestures from speech audio with conditional variational autoencoders," in *Proceedings of the IEEE/CVF International Conference on Computer Vision*, 2021, pp. 11 293–11 302.
- [37] S. Yang, Z. Wu, M. Li, Z. Zhang, L. Hao, W. Bao, M. Cheng, and L. Xiao, "Diffusestylegesture: Stylized audio-driven co-speech gesture generation with diffusion models," *arXiv preprint arXiv:2305.04919*, 2023.
- [38] L. Zhu, X. Liu, X. Liu, R. Qian, Z. Liu, and L. Yu, "Taming diffusion models for audio-driven co-speech gesture generation," in *Proceedings of the IEEE/CVF Conference on Computer Vision and Pattern Recognition*, 2023, pp. 10 544–10 553.
- [39] T. Ao, Z. Zhang, and L. Liu, "Gesturediffuclip: Gesture diffusion model with clip latents," *ACM Transactions on Graphics (TOG)*, vol. 42, no. 4, pp. 1–18, 2023.
- [40] X. Liu, Q. Wu, H. Zhou, Y. Xu, R. Qian, X. Lin, X. Zhou, W. Wu, B. Dai, and B. Zhou, "Learning hierarchical cross-modal association for co-speech gesture generation," in *Proceedings of the IEEE/CVF Conference on Computer Vision and Pattern Recognition*, 2022, pp. 10 462–10 472.
- [41] I. Habibie, W. Xu, D. Mehta, L. Liu, H.-P. Seidel, G. Pons-Moll, M. Elgharib, and C. Theobalt, "Learning speech-driven 3d conversational gestures from video," in *Proceedings of the 21st ACM International Conference on Intelligent Virtual Agents*, 2021, pp. 101–108.
- [42] H. Wu and M. Flierl, "Learning product codebooks using vector-quantized autoencoders for image retrieval," in *2019 IEEE Global Conference on Signal and Information Processing (GlobalSIP)*. IEEE, 2019, pp. 1–5.
- [43] Y. Zhu, J. Feng, C. Zhao, M. Wang, and L. Li, "Counter-interference adapter for multilingual machine translation," *arXiv preprint arXiv:2104.08154*, 2021.
- [44] T. Lei, J. Bai, S. Brahma, J. Ainslie, K. Lee, Y. Zhou, N. Du, V. Zhao, Y. Wu, B. Li *et al.*, "Conditional adapters: Parameter-efficient transfer learning with fast inference," *Advances in Neural Information Processing Systems*, vol. 36, 2024.
- [45] X. L. Li and P. Liang, "Prefix-tuning: Optimizing continuous prompts for generation," *arXiv preprint arXiv:2101.00190*, 2021.
- [46] X. Liu, K. Ji, Y. Fu, W. L. Tam, Z. Du, Z. Yang, and J. Tang, "P-tuning v2: Prompt tuning can be comparable to fine-tuning universally across scales and tasks," *arXiv preprint arXiv:2110.07602*, 2021.
- [47] E. J. Hu, Y. Shen, P. Wallis, Z. Allen-Zhu, Y. Li, S. Wang, L. Wang, and W. Chen, "Lora: Low-rank adaptation of large language models," *arXiv preprint arXiv:2106.09685*, 2021.
- [48] A. Edalatii, M. Tahaei, I. Kobzyev, V. P. Nia, J. J. Clark, and M. Rezagholizadeh, "Krona: Parameter efficient tuning with kronecker adapter," *arXiv preprint arXiv:2212.10650*, 2022.
- [49] N. Houlsby, A. Giurgiu, S. Jastrzebski, B. Morrone, Q. De Laroussilhe, A. Gesmundo, M. Attariyan, and S. Gelly, "Parameter-efficient transfer learning for nlp," in *International conference on machine learning*. PMLR, 2019, pp. 2790–2799.
- [50] J. He, C. Zhou, X. Ma, T. Berg-Kirkpatrick, and G. Neubig, "Towards a unified view of parameter-efficient transfer learning," *arXiv preprint arXiv:2110.04366*, 2021.
- [51] R. Rombach, A. Blattmann, D. Lorenz, P. Esser, and B. Ommer, "High-resolution image synthesis with latent diffusion models," in *Proceedings of the IEEE/CVF conference on computer vision and pattern recognition*, 2022, pp. 10 684–10 695.
- [52] Y. Li, H. Liu, Q. Wu, F. Mu, J. Yang, J. Gao, C. Li, and Y. J. Lee, "Gligen: Open-set grounded text-to-image generation," in *Proceedings of the IEEE/CVF Conference on Computer Vision and Pattern Recognition*, 2023, pp. 22 511–22 521.
- [53] L. Zhang, A. Rao, and M. Agrawala, "Adding conditional control to text-to-image diffusion models," in *Proceedings of the IEEE/CVF International Conference on Computer Vision*, 2023, pp. 3836–3847.
- [54] C. Mou, X. Wang, L. Xie, Y. Wu, J. Zhang, Z. Qi, and Y. Shan, "T2i-adapter: Learning adapters to dig out more controllable ability for text-to-image diffusion models," in *Proceedings of the AAAI Conference on Artificial Intelligence*, vol. 38, no. 5, 2024, pp. 4296–4304.
- [55] R. Gal, Y. Alaluf, Y. Atzmon, O. Patashnik, A. H. Bermano, G. Chechik, and D. Cohen-Or, "An image is worth one word: Personalizing text-to-image generation using textual inversion," *arXiv preprint arXiv:2208.01618*, 2022.
- [56] H. Ye, J. Zhang, S. Liu, X. Han, and W. Yang, "Ip-adapter: Text compatible image prompt adapter for text-to-image diffusion models," *arXiv preprint arXiv:2308.06721*, 2023.
- [57] Y. Gan, Z. Yang, X. Yue, L. Sun, and Y. Yang, "Efficient emotional adaptation for audio-driven talking-head generation," in *Proceedings of the IEEE/CVF International Conference on Computer Vision*, 2023, pp. 22 634–22 645.
- [58] A. Ramesh, P. Dhariwal, A. Nichol, C. Chu, and M. Chen, "Hierarchical text-conditional image generation with clip latents," *arXiv preprint arXiv:2204.06125*, vol. 1, no. 2, p. 3, 2022.
- [59] Z. Chang, W. Hu, Q. Yang, and S. Zheng, "Hierarchical semantic perceptual listener head video generation: A high-performance pipeline," in *Proceedings of the 31st ACM International Conference on Multimedia*, 2023, pp. 9581–9585.
- [60] M. Sun, C. Xu, X. Jiang, Y. Liu, B. Sun, and R. Huang, "Beyond talking—generating holistic 3d human dyadic motion for communication," *arXiv preprint arXiv:2403.19467*, 2024.
- [61] T. Ao, Q. Gao, Y. Lou, B. Chen, and L. Liu, "Rhythmic gesticulator: Rhythm-aware co-speech gesture synthesis with hierarchical neural embeddings," *ACM Transactions on Graphics (TOG)*, vol. 41, no. 6, pp. 1–19, 2022.
- [62] L. Muda, M. Begam, and I. Elamvazuthi, "Voice recognition algorithms using mel frequency cepstral coefficient (mfcc) and dynamic time warping (dtw) techniques," *arXiv preprint arXiv:1003.4083*, 2010.
- [63] A. Baeviski, Y. Zhou, A. Mohamed, and M. Auli, "wav2vec 2.0: A framework for self-supervised learning of speech representations," *Advances in neural information processing systems*, vol. 33, pp. 12 449–12 460, 2020.
- [64] S. Kum and J. Nam, "Joint detection and classification of singing voice melody using convolutional recurrent neural networks," *Applied Sciences*, vol. 9, no. 7, p. 1324, 2019.

- [65] V. Panayotov, G. Chen, D. Povey, and S. Khudanpur, "Librispeech: an asr corpus based on public domain audio books," in *2015 IEEE international conference on acoustics, speech and signal processing (ICASSP)*. IEEE, 2015, pp. 5206–5210.
- [66] J. Devlin, M.-W. Chang, K. Lee, and K. Toutanova, "Bert: Pre-training of deep bidirectional transformers for language understanding," *arXiv preprint arXiv:1810.04805*, 2018.
- [67] G. Tevet, B. Gordon, A. Hertz, A. H. Bermano, and D. Cohen-Or, "Motionclip: Exposing human motion generation to clip space," in *European Conference on Computer Vision*. Springer, 2022, pp. 358–374.
- [68] H. Wu, J. Jia, H. Wang, Y. Dou, C. Duan, and Q. Deng, "Imitating arbitrary talking style for realistic audio-driven talking face synthesis," in *Proceedings of the 29th ACM International Conference on Multimedia*, 2021, pp. 1478–1486.
- [69] Y. Yoon, B. Cha, J.-H. Lee, M. Jang, J. Lee, J. Kim, and G. Lee, "Speech gesture generation from the trimodal context of text, audio, and speaker identity," *ACM Transactions on Graphics (TOG)*, vol. 39, no. 6, pp. 1–16, 2020.
- [70] R. Li, S. Yang, D. A. Ross, and A. Kanazawa, "Ai choreographer: Music conditioned 3d dance generation with aist++," in *Proceedings of the IEEE/CVF International Conference on Computer Vision*, 2021, pp. 13 401–13 412.
- [71] X. Huang and S. Belongie, "Arbitrary style transfer in real-time with adaptive instance normalization," in *Proceedings of the IEEE international conference on computer vision*, 2017, pp. 1501–1510.